

indicates that the emitting state is atomic, or molecular, in character. Hence it has relatively small interaction with the surrounding lattice. This fact may indicate that there is a covalent type of bonding between the two  $Tl^+$  ions that make up the dimer center. The short lifetime and small Stokes shift indicate that the wave function of this center remains relatively closely confined to the immediate vicinity of the dimer center, in contrast to that of the monomer center. This is analogous to the short lifetime of the  $M$  center (two  $F$  centers) as opposed to the relatively long lifetime of  $F$ -center luminescence as reported by Swank and Brown<sup>14</sup> and discussed by Fowler.<sup>15</sup>

<sup>14</sup> R. A. Swank and F. C. Brown, *Phys. Rev.* **130**, 34 (1963).

<sup>15</sup> W. Beall Fowler, *Phys. Rev.* **135**, A1725 (1964).

A basic consequence of the  $\langle 100 \rangle$  orientation of the dimer center is the fact that the two  $Tl^+$  ions are not in nearest-neighbor positions. As of now, it is not possible to answer the question of what is in between them; but, whatever it is, it is felt that it plays an essential role in the mechanism by which dimers are formed and held together.

#### ACKNOWLEDGMENTS

We wish to express our thanks to Donald Beck for writing the computer program for the lifetime measurement and to Dr. W. Beall Fowler for some very helpful discussions. We also wish to thank the Harshaw Chemical Co. for providing us with our samples.

## Lattice Sidebands of Vibrational Spectra and Their Pressure Dependence

M. A. CUNDILL AND W. F. SHERMAN

*Department of Physics, King's College, London, England*

(Received 11 October 1967)

Vibrational spectra of solids which show the general form  $\nu_{\text{int}} \pm \nu_{\text{ext}}$  are discussed, and the information that they contain about the lattice modes of the solid is considered. Small polyatomic impurity ions isolated in alkali halides are responsible for most of the spectra considered. The importance of torsional motion of the impurity ion is shown, and a directional selection of  $\nu_{\text{ext}}$  controlled by the  $\nu_{\text{int}}$  transition moment is suggested. The pressure dependence of some of these spectra, up to 50 kbar at 100°K, is presented and discussed in terms of the host-lattice dispersion curves. For instance, it is shown that there is no acoustic-to-optic energy gap in the high-pressure CsCl-type structures of KBr, KI, RbBr, and RbI. Some of the wider applications of this type of spectrum are also indicated.

#### INTRODUCTION

VIBRATIONAL spectra which have the general form  $\nu_{\text{int}} \pm \nu_{\text{ext}}$  have been reported for several different systems, e.g., iodoform,<sup>1</sup> brucite,<sup>2</sup> polyatomic impurity ions in alkali halides,<sup>3-6</sup> impurity molecules in solidified rare-gas matrices.<sup>7</sup>  $\nu_{\text{int}}$  is a frequency which

<sup>1</sup> R. M. Hexter and H. Cheung, *J. Chem. Phys.* **24**, 1187 (1956).

<sup>2</sup> R. M. Hexter, *J. Opt. Soc. Am.* **48**, 770 (1958).

<sup>3</sup> J. C. Decius, J. L. Jacobson, W. F. Sherman, and G. R. Wilkinson, *J. Chem. Phys.* **43**, 2180 (1965).

<sup>4</sup> R. Metselaar and J. van der Elsken, *Phys. Rev. Letters* **16**, 349 (1966).

<sup>5</sup> M. A. Cundill and W. F. Sherman, *Phys. Rev. Letters* **16**, 570 (1966).

<sup>6</sup> C. K. Chau, M. V. Klein, and B. Wedding, *Phys. Rev. Letters* **17**, 521 (1966).

<sup>7</sup> B. Vodar, in Fourth High-Pressure Research Meeting, Eindhoven, 1966 (unpublished). Although there are many references available in the published literature which give spectra of impurities isolated in rare-gas matrices [e.g., L. F. Keyser and G. W. Robinson, *J. Chem. Phys.* **44**, 3225 (1966); D. E. Mann, N. Acquista, and D. White, *ibid.* **44**, 3453 (1966)], there do not seem to be any examples which show a very strong  $Q$  branch accompanied by sum and difference binary combinations with the host crystal lattice vibrations. We understand, however, that this type of spectrum has been observed in Professor B. Vodar's laboratory, Bellevue, France.

can be identified with a specific molecular group and which occurs at an energy only slightly displaced from that at which it would be found in an isolated molecule.  $\nu_{\text{ext}}$  are frequencies associated with the movement of one molecule with respect to its neighbors, and represent a selection of the available energies of the lattice vibrations of the crystal at the point at which it is sampled. In iodoform, for example, if the C-H stretching frequency is used as  $\nu_{\text{int}}$  and the radiation passed through the crystal such that its  $E$  vector is perpendicular to the C-H bonds, all of which align in the crystal, then the sharp C-H absorption is itself seen only very weakly (only seen at all because of convergence of the beam, crystal imperfections, etc.), and broad wings are seen extending between 20 and 50  $\text{cm}^{-1}$  on each side. By cooling the crystal to liquid-helium temperature the low-energy wing can be completely suppressed. In principle, any strongly active band should show this kind of side structure, but the best examples are certainly those where complete longitudinal alignment of the  $\nu_{\text{int}}$  transition moment renders it virtually non-absorbing and allows the usually broad  $\pm \nu_{\text{ext}}$  bands to

be clearly seen right up to the center frequency, e.g., C-H bands of iodoform, O-H bands in  $\text{Mg}(\text{OH})_2$ , O-H bands in  $\text{Ca}(\text{OH})_2$ , and  $\text{CO}_3$  bands in calcite have been used in this way in this laboratory.<sup>8</sup> However, if a very strong band is exceptionally sharp, then only a little of the lowest-energy side structure is obscured by the main band. Very sharp, very strong bands can best be obtained by matrix isolation methods, and it is therefore not surprising that impurity molecules in rare-gas matrices, and impurity ions in alkali halides show good examples of  $\nu_{\text{int}} \pm \nu_{\text{ext}}$  spectra.

### IONS IN ALKALI HALIDES

The  $\nu_{\text{ext}}$  frequencies are such that they would occur directly in the far-infrared region of the spectrum, where alkali halides absorb very strongly; see, for example, the absorption of KI shown in Fig. 1. However, the absorption spectra associated with at least 12 different impurity ions isolated in KI have been recorded directly in the far infrared.<sup>9,10</sup> In some, if not all, of these cases there is as much impurity activated absorption which has not been detected because of the very strong host-lattice absorption. When investigating the external motion of polyatomic ions isolated in alkali halides, there are several advantages to be gained from studying the binary combination of this motion with a suitable internal mode, rather than observing the fundamental absorption in the far infrared. Firstly, the entire range of external-mode energies is unobscured. Secondly, the external modes can be studied over a wide range of temperatures. Thirdly, the internal mode can be chosen to occur in a spectral region where subsidiary tech-

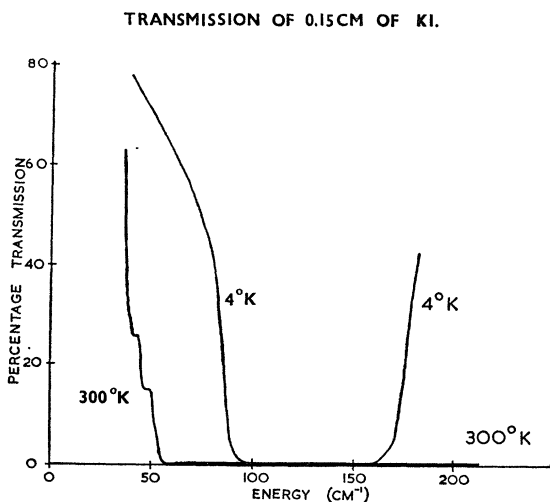


FIG. 1. Far-infrared transmission spectrum of a 1.5-mm-thick crystal of KI at room temperature and at 4°K.

<sup>8</sup> See, e.g., Final Technical Reports on U. S. Army Contract Nos. DA-91-591-EUC-1308 (unpublished).

<sup>9</sup> K. F. Renk, Phys. Letters 14, 281 (1965).

<sup>10</sup> A. J. Sievers, A. A. Maradudin, and S. S. Jaswal, Phys. Rev. 138, A272 (1965).

niques, in our case the use of high-pressure cells, are much more straightforward. Fourthly, features in  $\nu_{\text{int}} \pm \nu_{\text{ext}}$  spectra are unambiguously associated with the ion responsible for  $\nu_{\text{int}}$ , which makes it possible to obtain at least some of the relevant information from samples containing more than one impurity (i.e.,  $\text{NCO}^-$  contained in  $\text{CN}^-$ - or  $\text{NCS}^-$ -doped crystals,  $\text{NO}_2^-$  contained in  $\text{NO}_3^-$ -doped crystals, etc.).

A disadvantage of using the binary combination spectra is that they are relatively weak, which is only partially compensated for by the increased sample thickness that can be used. Typically, doping concentrations of between 0.1 and 1.0% have been used, compared with the 0.01% which has usually been found to be sufficient for the direct observation of the external-mode absorption in the far infrared. Although concentrations as high as 1% can be expected, in some cases<sup>11</sup> to cause distortion of the spectra from that to be expected from a very dilute solution, none of our spectra was found to show any concentration dependence. The identification of genuine external-mode absorption from any other weak absorptions in the vicinity of the internal mode is greatly assisted by the temperature dependence of the difference band features.

There still remains the problem of the rules governing the intensity of the various features seen in direct absorption in the far infrared, and in binary combination with an internal mode in the near infrared. Even where there is insufficient symmetry to render inactive any of the modes in either region, the relative intensities of different modes as observed directly or in combination with  $\nu_{\text{int}}$  may vary greatly. It is clearly advisable to investigate both regions if the external vibrations of the impurity are to be better understood.

Consider, for instance, a  $\text{BO}_2^-$  ion ( $D_{\infty h}$ ) present as a substitutional impurity in a NaCl-type lattice ( $O_h$ ) and oriented in a  $\langle 111 \rangle$  direction. The local symmetry is  $D_{3d}$  and, as first pointed out to us by Decius,<sup>12</sup> out of the distinct rigid-body modes ( $T_z$  in  $A_{2u}$ ,  $T_x$  and  $T_y$  in  $E_u$ , and  $R_x$  and  $R_y$  in  $E_g$ ) only  $R_x$  and  $R_y$  can give infrared activity in binary combination with  $\nu_3$  ( $A_{2u}$ ), and these are the modes which are inactive in the far infrared as fundamentals. There is also the possibility of infrared active binary combinations with the other two internal modes. Such combinations with  $\nu_2$  would have similar rules to those with  $\nu_3$ , but if the active combinations with  $\nu_1$ , the infrared inactive symmetric stretch, could be found, then they would show the translational modes in exactly the same form as the direct observations in the far infrared. Apart from the above rigid-body modes, there is the ability of the molecular impurity ion occupied lattice site to absorb energy, which for a pure lattice is associated with a propagating lattice mode. This can be justified by the same arguments as used for point impurities, but the charge distribution of a molecular impurity ion (dipole, or at least extended

<sup>11</sup> G. Benedek and G. F. Nardelli, Phys. Rev. 155, 1004 (1967).

<sup>12</sup> J. C. Decius (private communication).

quadrupole) and the transition moment of  $\nu_{\text{int}}$  define directions within the crystal, in contrast to the point impurity system. Thus, although all modes will in general be allowed, in the sense that they are not forbidden by any selection rules, it is to be expected that the relative intensities with which they appear, both directly and in binary combination with  $\nu_{\text{int}}$  (vibrational, or electronic), will vary considerably, just as the intensities of the various allowed internal modes are found to vary considerably.

$\nu_{\text{int}} \pm \nu_{\text{ext}}$  spectra for a variety of ions in up to 12 different alkali halides will now be presented. The type of impurity ion motion to be associated with specific features in  $\nu_{\text{ext}}$  will be considered, as will the relevance of impurity-ion axis orientation, and an indication will be given of the information which can be obtained from the pressure dependence of these spectra.

### NCO<sup>-</sup> IN KBr

Figure 2 shows the  $\nu_3 \pm \nu_{\text{ext}}$  spectrum for NCO<sup>-</sup> isolated in KBr compared with the dispersion curves of the lattice vibrations of KBr at 90°K obtained from neutron-scattering experiments.<sup>13</sup> This was the first impurity ion spectrum of this kind which we investigated (see Ref. 3), and the four relatively sharp lines to be seen in  $\nu_{\text{ext}}$  make it an attractive spectrum with which to work. Dispersion curves have been used in

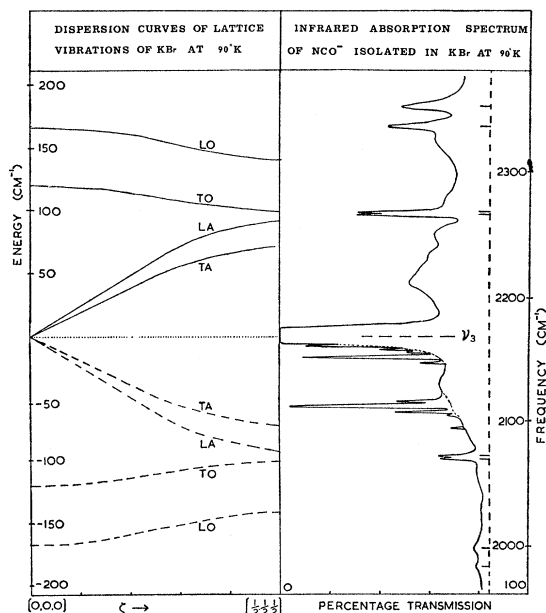


FIG. 2. Absorption spectrum of NCO<sup>-</sup> isolated in KBr, showing the external-mode vibrations in sum and difference combination with  $\nu_3$  compared with the (111) dispersion curves of the lattice vibrations of pure KBr. The sharp, dotted-under features to the low-energy side of the main  $\nu_3$  absorption line are due to small traces of the various isotopic species of NCO<sup>-</sup> as they occur in natural abundance. (See Ref. 3.)

<sup>13</sup> A. D. B. Woods, B. N. Brockhouse, R. A. Cowley, and W. Cochran, Phys. Rev. 131, 1025 (1963).

### LOCAL MODE FREQUENCIES AT 100°K OF NCO<sup>-</sup> ISOLATED IN KBr

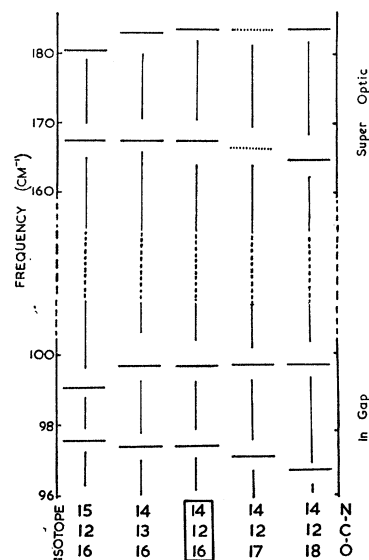


FIG. 3. External local-mode frequencies found in combination with  $\nu_3$ (NCO<sup>-</sup>) isolated in KBr for the various isotopic species.

Fig. 2, because it is believed that this type of presentation shows most clearly the interrelation of the  $\nu_{\text{ext}}$  spectra with the host-lattice properties. It is not intended to suggest that preferential combination takes place with lattice vibrations which propagate in any particular direction, or even that the radiant energy is directly transformed into propagating modes, although it is quickly dissipated via such modes.

In Ref. 3, the C<sup>12</sup>-to-C<sup>13</sup> shift in the four sharp bands shown in  $\nu_{\text{ext}}$  (see Fig. 2) was found to be very small. Since for a completely localized translational mode this shift would be just over 1 cm<sup>-1</sup> for lines at 97.4 and 99.7 cm<sup>-1</sup> and about 2 cm<sup>-1</sup> for bands at 167.5 and 183.6 cm<sup>-1</sup>, it was suggested that these bands did not represent highly localized vibrations. However, our trial calculations on the motion of polyatomic impurities suggest that in this case, and in many others, torsional oscillations are likely to produce the highest-energy (and therefore most clearly resolved) localized modes.

In this type of motion, the isotopic mass of the center nucleus is relatively unimportant, and for this reason we decided to investigate the effects of the other isotopic substitutions that were possible with the NCO<sup>-</sup> ion.

Figure 3 shows schematically the sharp external-mode frequency data collected for the isotopically different species of NCO<sup>-</sup> ions isolated in KBr.

Although very high purity isotopically enriched samples are available, the data presented in Fig. 3 refer to samples which contain only partial enrichment. This allowed the separation of peaks to be measured for two different species in the same sample, at the same

TABLE I. Isotopic frequency shifts (in  $\text{cm}^{-1}$ ) of sharp external-mode features found in combination with  $\nu_8(\text{NCO}^-)$  isolated in KBr. The observed values are compared with values calculated on the assumption of pure torsional modes within an infinitely massive containing well, about two axes perpendicular to the ion axis, one bisecting the N-C bond and the other bisecting the C-O bond. Figures in brackets represent  $\text{calc}\Delta\nu/\text{scaling factor}$ .

$(\nu_{\text{int}} + \nu_{\text{ext}}) - \nu_{\text{int}}$ $\text{N}^{14}\text{C}^{12}\text{O}^{16}$	97.4 $\text{cm}^{-1}$	99.7 $\text{cm}^{-1}$	167.5 $\text{cm}^{-1}$	183.6 $\text{cm}^{-1}$	
$\Delta\nu(14,12,16)-(15,12,16)$	-0.2 0.2(0.03)	0.6 2.5(0.62)	$\sim 0$ 0.5(0.2)	3 4 (3.0)	obs. calc.
$\Delta\nu(14,12,16)-(14,13,16)$	0 0.2(0.03)	0 0.2(0.05)	$\sim 0$ 0.4(0.16)	0.4 0.4(0.3)	obs. calc.
$\Delta\nu(14,12,16)-(14,12,17)$	0.3 2.5(0.34)	$\sim 0$ 0.3(0.07)	$\sim 1.5$ 4 (1.6)	$\sim 0$ 0.5(0.37)	obs. calc.
$\Delta\nu(14,12,16)-(14,12,18)$	0.7 5 (0.71)	$\sim 0$ 0.6(0.15)	3 8 (3.2)	$\sim 0$ 1 (0.7)	obs. calc.
Estimated reliability of observed frequency shifts	$\pm 0.15$	$\pm 0.15$	$\pm 0.3$	$\pm 0.3$	
Scaling (delocalization) factor	$\sim 7$	$\sim 4$	$\sim 2\frac{1}{2}$	$\sim 1\frac{1}{3}$	

temperature on the same spectrum. A spectral resolution of better than  $1 \text{ cm}^{-1}$  was used with a precision of about  $\pm 0.1 \text{ cm}^{-1}$ , but we only feel justified in quoting values for centers of the broader, superoptic bands to an accuracy of about  $\pm 0.2 \text{ cm}^{-1}$ . This means that with the possible exception of the  $97.4\text{--}97.6\text{-cm}^{-1}$  shift for  $\text{N}^{15}$  substitution, the frequency changes shown in Fig. 3 are all unambiguously established. The samples used were about 1 cm along the radiation path and about 6 mm by 4 mm in cross section. They were grown from the melt with total  $\text{NCO}^-$  doping of about 0.8% anion replacement, and were apparently completely homogeneous.

If the features referred to in Fig. 3 are described as a sharp in-the-gap doublet, and a broader superoptic doublet, then it can be seen that oxygen substitution effects only the lower component of each doublet, while nitrogen substitution effects primarily the upper components, and carbon substitution has very little effect on any of these bands. There would appear to be only one plausible expansion of these shifts. The motion of the  $\text{NCO}^-$  ion is predominantly torsional in all four cases. The  $97.4\text{-cm}^{-1}$  and  $167.5\text{-cm}^{-1}$  bands involve large oxygen movement and small carbon and nitrogen movement, and thus represent torsion about an axis cutting the  $\text{NCO}^-$  ion somewhere along the C-N bond. The  $99.7\text{-cm}^{-1}$  and  $183.6\text{-cm}^{-1}$  bands involve large nitrogen movement and therefore represent torsion about an axis cutting the C-O bond. It remains to distinguish between the in-the-gap modes and the superoptic modes in terms of the part played by the environment.

What information is available about the part played by the environment? Consider first the magnitude of the observed frequency shifts compared with the values obtained from the simplest possible calculation of such shifts. Table I shows this comparison. The assumptions made in the calculation are: (i) The  $\text{NCO}^-$  ion is treated as rigid; (ii) the N-C spacing is taken equal to the C-O spacing within the  $\text{NCO}^-$  ion; (iii) the  $97.4\text{-cm}^{-1}$  and  $167.5\text{-cm}^{-1}$  bands result from torsional motion about an axis which perpendicularly bisects the C-N bond; (iv) the

$99.7\text{-cm}^{-1}$  and  $183.6\text{-cm}^{-1}$  bands represent torsional motion about an axis which perpendicularly bisects the C-O bond; (v) the motion takes place within an infinitely massive containing potential well. (This ignores the fact that these could not all be normal vibrations of such an oversimplified system.<sup>14</sup>)

The general form of the table of calculated values can be seen to result immediately from the fact that the sensitivity to mass change of a given oscillation is nine times greater for the nucleus farthest from its torsional axis than it is for either of the other two. These calculated shifts are all inevitably too large, but if a scaling factor is associated with each absorption band, then agreement between calculated and observed shifts (within the experimental errors) is easily obtained. The scaling factors required are included at the foot of Table I, and indicate the extent of the environmental participation in the motion. Thus for the  $97.4\text{-cm}^{-1}$  band 6/7 of the energy is associated with motion of the environment and only 1/7 with motion of the  $\text{NCO}^-$  ion, whereas for the  $183.6\text{-cm}^{-1}$  band only  $\frac{1}{4}$  of the energy is associated with the environment and  $\frac{3}{4}$  with the  $\text{NCO}^-$  ion. This scaling, or delocalization, factor would be infinite for a completely delocalized mode and unity for a completely localized mode.

These delocalization factors show that the superoptic modes are more localized than the in-the-gap modes, and for both doublets the higher-energy component (large nitrogen amplitude) is more localized than the lower-energy component (large oxygen amplitude).

Calculations on the force constants operating between the  $\text{NCO}^-$  and its neighbors show that the bulk of the restoring force acting on an  $\text{NCO}^-$  rotated out of its  $\langle 111 \rangle$  equilibrium orientation comes from the two rings of three nearest neighbors between which it can be regarded as being held (see Fig. 4). If only the nearest-neighbor restoring force is considered, and the ratio

<sup>14</sup> A fairly simple system which would be capable of all these modes is obtained if each of the three  $\text{NCO}^-$  nuclei is surrounded by a ring (of neighboring ions moving together), when out of the 27 deg of freedom, eight (four double degenerate modes) involve large torsional motion of the  $\text{NCO}^-$ .

of the nearest-neighbor amplitude to that of the nitrogen nucleus is called  $\alpha$  for the vibration responsible for the  $183.6\text{-cm}^{-1}$  absorption and  $\beta$  for the  $99.7\text{-cm}^{-1}$  band, then the following relationship can be derived:  $(183.6/99.7)^2 = (1-\alpha)/(1-\beta)$ . (All motion has been considered to be in a direction parallel to the plane in which the  $\text{NCO}^-$  oscillates.) Since both  $\alpha$  and  $\beta$  must be small numbers ( $-0.20 < \alpha < 0.20$  and  $-0.42 < \beta < 0.42$ ) to stay within the observed degree of localization, then  $\alpha$  can be seen to be a small negative number and  $\beta$  can be seen to be a small positive number.<sup>15</sup> Thus, the three nearest neighbors must move with the nitrogen nucleus during the  $99.7\text{-cm}^{-1}$  vibration and against it in the  $183.6\text{-cm}^{-1}$  vibration. A similar result is obtained for the near neighbors to the oxygen nucleus for the other two bands, at  $97.4$  and  $167.5\text{ cm}^{-1}$ .

The nature of the vibrations associated with the four bands can now be more fully described. The  $97.4\text{-cm}^{-1}$  band is due to torsional oscillations of the  $\text{NCO}^-$  ion about an axis perpendicularly dividing the N-C bond, accompanied by an in-phase (acoustical) movement of the three potassium ion forming a ring round the oxygen nucleus of the  $\text{NCO}^-$  ion. The  $99.7\text{-cm}^{-1}$  band corresponds to a large nitrogen amplitude acoustic torsional mode. The  $167.5\text{-cm}^{-1}$  band is due to a large oxygen amplitude optical torsion and the  $183.6\text{-cm}^{-1}$  band is due to a large nitrogen amplitude optical torsion.

Only the three nearest neighbors to the large amplitude nucleus of the  $\text{NCO}^-$  ion are being referred to when the terms "acoustic" and "optic" are used in the above description. Figure 5 shows schematically the four vibrations as described above. It is possible,

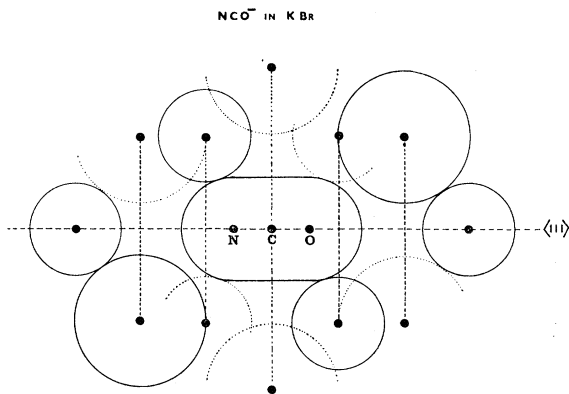


FIG. 4. Schematic presentation of the KBr environment surrounding an  $\text{NCO}^-$  present as a substitutional impurity with its axis orientated in a  $\langle 111 \rangle$  direction is drawn to scale using Goldschmidt radii. The small circles represent  $\text{K}^+$  ions, the large circles  $\text{Br}^-$  ions. Ions in the plane of the paper are presented as solid circles, ions out of this plane are shown dotted. Note particularly how the  $\text{NCO}^-$  is held between two rings of  $\text{K}^+$  ions, each composed of one ion in the plane of the paper and two out of this plane.

<sup>15</sup>  $\alpha$  could only go positive if  $\beta$  were made greater than  $0.705$ , or  $\beta$  negative if  $\alpha$  were taken more negative than  $-2.39$ ; these two possibilities are outside the admissible range.

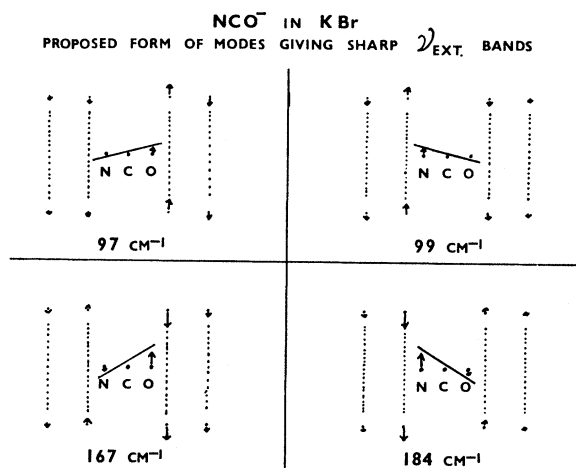


FIG. 5. Proposed form of the vibrations giving sharp bands in the external-mode spectrum of  $\text{NCO}^-$  isolated in KBr. The dotted lines represent the planes of nearest and next nearest neighbors illustrated in Fig. 4.

starting with the diagrams of Fig. 5, to calculate amplitude envelope functions which decay exponentially with distance from the large amplitude  $\text{NCO}^-$  nucleus such that the vibrations depicted have about the observed delocalization factors, while satisfying the requirements of no-net translation and zero-net angular momentum. A small percentage of the motion of some of the ions is required to be nonparallel to the plane in which the  $\text{NCO}^-$  ion oscillates.

Several points mentioned earlier are illustrated in the diagrams of Fig. 5. Firstly, the degree of delocalization of the acoustic-type modes was found to be greater than their corresponding optic-type modes (factors of  $7$  and  $4$  compared with  $2\frac{1}{2}$  and  $1\frac{1}{3}$ ; see Table I). The requirement of stationary c.m. could ideally be satisfied by the nearest neighbors alone for the optic-type modes, whereas in the acoustic-type modes at least the next nearest neighbors are required. It soon becomes apparent when making calculations on the models illustrated in Fig. 5, that the optic-type modes for this system are inevitably going to be more highly localized than the corresponding acoustic modes.

Secondly, the fact that all four sharp features in the  $\nu_{\text{ext}}$  spectrum, shown in Fig. 2, are being attributed to localized torsional modes is seen to be quite reasonable. A calculation of the somewhat similar modes involving translation of the  $\text{NCO}^-$  ion results in appreciably lower frequencies. Essentially, this is because the whole  $\text{NCO}^-$  mass vibrates against the environment in the translational modes, whereas effectively only one end is concerned in the torsional case. Thus it is to be expected that modes involving torsion of this impurity ion will find it easiest to rise in frequency, sufficiently to come clear of the corresponding lattice band and appear as sharp localized absorptions.

This pattern of localized acoustic- and optic-type torsional modes which we have justified above for the

case of  $\text{NCO}^-$  in KBr we believe to be a general feature of many polyatomic impurity ion in alkali-halide  $\nu_{\text{ext}}$  spectra.

The proposed torsional nature of these modes would explain why when  $\text{N}_3^-$  or  $\text{BO}_2^-$  is used in KBr as the source of  $\nu_{\text{int}}$ , only one in-the-gap and one superoptic mode is seen. (See Refs. 3 and 5.) In these cases, as was mentioned earlier, it is the torsional modes ( $R_x, R_y$ ) that are expected to be active in combination with  $\nu_3$ .<sup>16</sup>

If  $\text{NO}_2^-$  or  $\text{NO}_3^-$  (see Refs. 4, 5, and 9) or any other nonlinear ion is used, an increased number of lines becomes possible in terms of torsional motion about different axes.

Since the torsional motion of the ions seemed likely to be playing an important part in at least some of the sharper features in the  $\nu_{\text{ext}}$  spectra of polyatomic impurity ions in alkali halides, it was decided that the  $\nu_{\text{ext}}$  spectra for ions suspected of hindered rotation<sup>17-19</sup> should be further investigated. Reference 5 contains some of our earlier data on  $\nu_{\text{ext}}$  for  $\text{CN}^-$  in the sodium halides, where  $\nu_{\text{int}}$  was sharp enough at 90°K for the  $\nu_{\text{ext}}$  features to be seen virtually undistorted. In the sodium halides, the barriers to rotation of the  $\text{CN}^-$  ion are quite large,<sup>17,19</sup> and it is the corresponding spectra for this ion in the potassium, rubidium, or cesium halides where it is able to rotate relatively freely that are interesting in the present context. For  $\text{CN}^-$  isolated in these halides, however, it is necessary to work at temperatures of 15°K or below if  $\nu_{\text{int}}$  is to be reduced to a usable sharp line. At temperatures below 15°K the difference part of the spectrum ( $\nu_{\text{int}} - \nu_{\text{ext}}$ ) is almost completely suppressed, which is unfortunate from the point of view of checking the identification of features in the  $\nu_{\text{int}} + \nu_{\text{ext}}$  region. However, bands due to other impurities which might be found in the relevant region are unlikely to show the marked temperature dependence below 25°K that is expected of the spectra of interest. In all our heavily cyanide-doped crystals, there was at least a small amount of cyanate impurity also. Although  $\nu_3(\text{NCO}^-)$  is usually a very sharp band, its presence in these spectra is unfortunate in that it appears in the various alkali halides at 90-100  $\text{cm}^{-1}$  above the fundamental cyanide band, which is a region of considerable interest in many of the  $\nu_{\text{ext}}$  spectra.

### $\text{CN}^-$ IN KBr

Figure 6 shows the spectrum obtained from a 1-cm-long crystal of KBr at about 7°K, which was nominally

<sup>16</sup> However, the four sharp  $\text{NCO}^-$  bands must all be doubly degenerate and the two  $\text{N}_3^-$  bands would each be fourfold degenerate. Thus they cannot simply represent the rigid-body modes, but must include six degrees of freedom "borrowed" from the lattice modes.

<sup>17</sup> W. D. Seward and V. Narayanamurti, *Phys. Rev.* **148**, 463 (1966).

<sup>18</sup> V. Narayanamurti, W. D. Seward, and R. O. Pohl, *Phys. Rev.* **148**, 481 (1966).

<sup>19</sup> G. R. Field and W. F. Sherman, *J. Chem. Phys.* **47**, 2378 (1967).

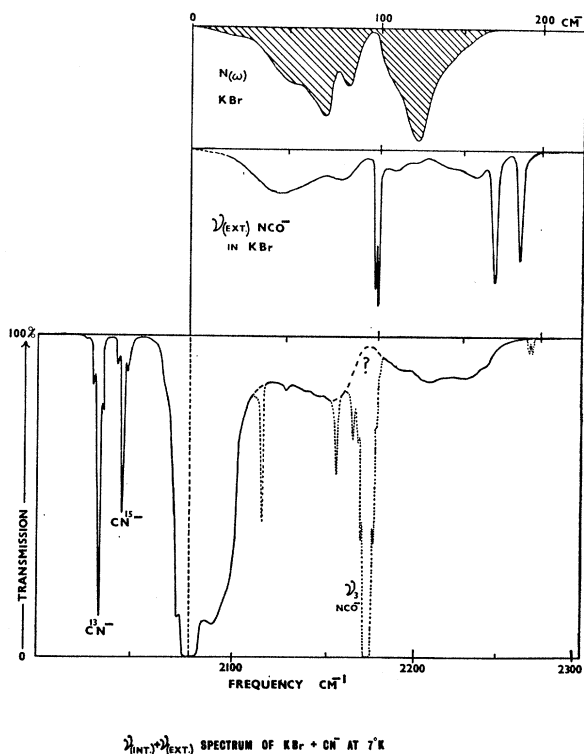


Fig. 6. 7°K absorption spectrum of  $\text{CN}^-$ -doped KBr. The external modes seen in combination with the C-N stretching mode ( $2078 \text{ cm}^{-1}$ ) of the  $(\text{C}^{12}\text{N}^{14})^-$  species are compared with the similar spectrum for  $\text{NCO}^-$  in KBr and the integrated density of states for KBr (see Ref. 13). Features due to  $\text{NCO}^-$  in the  $\text{CN}^-$ -doped crystal have been shown dotted.

doped with 0.8%  $\text{CN}^-$ . In this, the most heavily doped crystal that we used, almost 10% of the cyanide is estimated to have converted to cyanate.

The strong band at  $2078 \text{ cm}^{-1}$  is due to the stretching vibration of the  $(\text{C}^{12}\text{N}^{14})^-$  ion. Its strength can be gauged from the intensity of the less abundant isotopic species [i.e., it is approximately 90 times stronger than the  $(\text{C}^{13}\text{N}^{14})^-$  band]. The external-mode bands of interest in this figure are those seen in combination with the  $2078\text{-cm}^{-1}$  C-N stretching mode, and for comparison, the density of states of pure KBr<sup>13</sup> and the external modes found in combination with  $\nu_3(\text{NCO}^-)$  isolated in KBr have been drawn to the same scale, starting vertically above the  $2078\text{-cm}^{-1}$  line. Concentration-dependent satellites (see Ref. 3), which can be clearly seen on the low abundant isotopic species of the cyanide ion, are absorbing effectively 100% on the  $2078\text{-cm}^{-1}$  band and giving it an unnatural width. The greater transition probability<sup>19</sup> of the  $\nu_3(\text{NCO}^-)$  results in a peak absorbance ratio of only about 3:1 in favor of the  $\text{CN}^-$  bands in spite of the estimated 10:1 ratio in numbers.

First, consider the unobscured optic and superoptic regions of Fig. 6, where it can be seen that there are no sharp features in this spectrum. The acoustic to optic

mode gap is obscured in Fig. 6, but weaker samples, with better cyanide to cyanate ratios, showed no evidence of in-gap features of comparable intensity to those found for  $\text{NCO}^-$  [see Fig. 2 and the  $\nu_{\text{ext}}(\text{NCO}^-)$  spectrum plotted with respect to  $\nu(\text{CN}^-)$  for comparison in Fig. 6]. Figure 6 is further complicated in this "gap" region by the presence of concentration-dependent satellites on  $\nu_3(\text{NCO}^-)$  (see Ref. 3). For this sample, with a cyanide to cyanate ratio of about 10:1, the bulk of their structure is due to cyanide-cyanate pairs and is therefore different to that found in cyanate-only-doped crystals. In the present case, the satellites show increased structure at very low temperatures (below 20°K), which might be expected because the cyanide ion becomes frozen into some specific orientation with respect to the cyanate neighbor. Careful study of the available spectra leads us to believe that none of this absorption is due to  $\nu(\text{CN}^-) + \nu_{\text{ext}}$  in-the-gap modes. The growing of better crystals is under investigation, but even if it proves impossible to grow cyanate-free crystals with high-cyanide concentrations, the use of high-purity isotopic species would make it possible to investigate absorptions at this separation. [ $\text{C}^{13}$  shifts  $\nu_3(\text{NCO}^-)$  57  $\text{cm}^{-1}$  and  $\nu(\text{CN}^-)$  43  $\text{cm}^{-1}$ ;  $\text{N}^{15}$  shifts  $\nu_3(\text{NCO}^-)$  18  $\text{cm}^{-1}$  and  $\nu(\text{CN}^-)$  32  $\text{cm}^{-1}$ .]

The most striking difference between the  $\nu_{\text{ext}}$  spectra of  $\text{NCO}^-$  and  $\text{CN}^-$  each isolated in KBr is the absence in the  $\text{CN}^-$  spectrum of the four sharp lines which dominate the  $\text{NCO}^-$  spectrum. Since these have been assigned as localized torsional modes for the  $\text{NCO}^-$ , they were not expected for the  $\text{CN}^-$ , where the torsional restoring force is so small that bands of these energies cannot be obtained. Each spectrum shows basically two broad maxima within the acoustic band of KBr: at 44 and 80  $\text{cm}^{-1}$  for  $\text{NCO}^-$  and at 12.3 and 75  $\text{cm}^{-1}$  for  $\text{CN}^-$ . The feature at 12.3  $\text{cm}^{-1}$  in the cyanide spectrum has been reported<sup>17</sup> to sharpen considerably in going down to 2°K and is interpreted as the summation band involving the torsional oscillation of the  $\text{CN}^-$ , or, equivalently, as the  $T_{1u}(J=1)(v=0) \rightarrow T_{2g}(J=2)(v=1)$  transition of a vibrating hindered rotator obeying a Devonshire<sup>20</sup> model. Although this is a reasonably satisfactory explanation of the sharp band at 2°K (see, however, Ref. 15), the general broad absorption extending about 30  $\text{cm}^{-1}$  from the main line in Fig. 6 cannot be explained on the same model. Note also a residual absorption at about -12 to -15  $\text{cm}^{-1}$  from the main band which appears to be simply a thermally suppressed difference band equivalent (suggesting a sample temperature of about 6.5°K). The bulk of this absorption must, we believe, be due to combination with acoustic-type lattice vibrations in which the  $\text{CN}^-$  ion plays an energetically minor part. This is to be contrasted with the above models for the sharp band seen at 2°K at about  $\nu(\text{CN}^-) + (12 \text{ cm}^{-1})$ , where the energy is assumed to reside on the ion performing a specific

motion within an infinitely massive containing potential well. If an analogy is to be drawn between the low-separation absorption in the cyanide spectrum with the absorption showing a maximum at 44  $\text{cm}^{-1}$  in the cyanate spectrum, then the possible reasons for its changed position might be (i) different mass of impurity, (ii) different force constants between impurity and lattice, and (iii) different orientation of impurity within the lattice. The impurity mass is certainly not the dominant factor, since the heavier mass has the greater frequency. Also, since only a small fraction of the total energy is to be associated with the impurity in these essentially delocalized acoustic-type modes, the impurity mass is a parameter to which they might be expected to be insensitive. Calculations on the force constants operative in the two cases certainly show the  $\text{NCO}^-$  ion to be held more securely in a transverse and particularly a torsional sense, but both are held comparably longitudinally, and the transverse and longitudinal force constants are comparable to, or larger than, the host-lattice force constants. Again the proposed delocalized acoustic nature of the proposed modes would render them relatively insensitive to the local force constants,<sup>21,22</sup> although here at least the change from  $\text{CN}^-$  to  $\text{NCO}^-$  gives an effect in the observed direction, particularly for torsional motion. The effect of orientation is hard to assess, but it seems inevitable that if a given impurity ion were to be rotated into a different orientation within the crystal, then this would (a) change the local density of states, and (b) change the relative activity of the various modes as they appear in binary combination with  $\nu_{\text{int}}$ . It should be re-emphasized that the  $\nu_{\text{ext}}$  spectra observed here represent only a *selection* of the external modes involving the impurity, governed by the relative activity of these modes in binary combination with  $\nu_{\text{int}}$ . Similarly, the direct observation of external modes in the far infrared samples the total external-mode motion in terms of the fundamental infrared activity of these modes. Thus we believe that the orientation  $\langle 111 \rangle$  for  $\text{NCO}^-$  and  $\langle 001 \rangle$  for  $\text{CN}^-$  may well represent the overriding consideration for these low-energy

<sup>21</sup> Note the difference here between our low-energy broad bands and the sharp-resonance type of low-energy band observed for certain monatomic impurities (e.g.,  $\text{Li}^+$  in KBr). (See Ref. 22.) Benedek and Nardelli (Ref. 11) have made a theoretical investigation of the monatomic-impurity case and found that the sharp-resonant band part of the absorption is very sensitive to small changes in the force constant between the impurity and its nearest neighbors. The resonant mode is only so sensitive to force-constant changes because of the very small net-force constant which is operative in the examples which they quote, and the corresponding high degree of localization of the motion associated with this resonance which is shown by the large isotopic shift. In the  $\text{NCO}^-$  and  $\text{CN}^-$  cases, the force constants are comparable to, or larger than, those operative between host-lattice ions, and the observed low-energy absorption in these cases is more like the nonresonant part of the monatomic-impurity absorption, which on the Benedek and Nardelli model is described as "structures due to the host-lattice dynamics," which, not surprisingly, they find is insensitive to changes in the impurity ion's nearest-neighbor force constant.

<sup>22</sup> A. J. Sievers and S. Takeno, Phys. Rev. **140**, A1030 (1965).

<sup>20</sup> A. F. Devonshire, Proc. Roy. Soc. (London) **A153**, 601 (1936).

acoustic-type  $\nu_{\text{ext}}$ . This being so, it may be relevant to mention that zone-boundary values for the TA mode in pure KBr (see Ref. 13) vary from 40 to 74  $\text{cm}^{-1}$  for different reciprocal lattice directions. The LA, TO, and LO of pure KBr do not show such a marked directional dependence in the energies at which their dispersion curves show regions, where their slopes tend to zero, which may be considered to tie in with the fact that the  $\text{CN}^-$  and  $\text{NCO}^-$   $\nu_{\text{ext}}$  spectra show maxima in the same general regions at greater separations from the main line.

We have dealt at some length with the  $\nu_{\text{ext}}$  spectra observed for  $\text{NCO}^-$  and  $\text{CN}^-$  in KBr in order to establish the importance of torsional motion and to introduce the idea of directional dependence. We now consider other spectra in the light of these two concepts.

### $\nu_3 \pm \nu_{\text{ext}}$ SPECTRA FOR $\text{NCO}^-$ IN 12 ALKALI HALIDES

Figure 7 shows the  $\nu_{\text{ext}}$  spectra observed in combination with  $\nu_3$  of  $\text{NCO}^-$  when this ion was isolated in 12 alkali halides. Although many of our observed  $\nu_{\text{ext}}$  peak absorption energies have already been published,<sup>5</sup> Table II contains for completeness the relevant  $\text{NCO}^-$  values for all lattices. The four most extensive spectra in Fig. 7 (NaCl, NaBr, KCl, and RbCl) show an additional band at about 2400  $\text{cm}^{-1}$ . This is the lowest-energy component of a fermi triplet,  $2\nu_1$ ,  $\nu_1 + 2\nu_2$ ,  $4\nu_2$ , and it is quite possible that the concentration-dependent broadening of this line in NaBr is in fact obscuring some relevant  $\nu_{\text{ext}}$  structure. The best available calculated density-of-state curves for the various pure host lattices have been included in Fig. 7 (from models

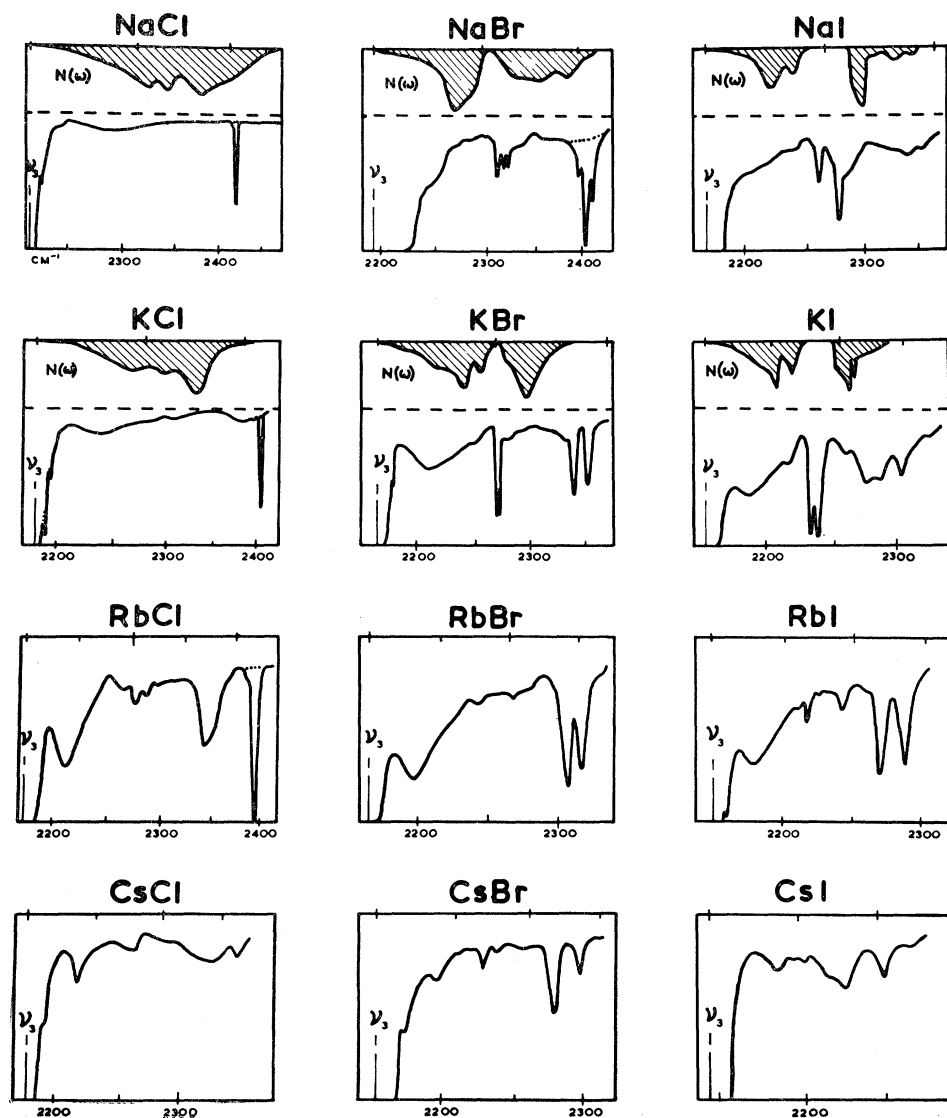


FIG. 7.  $\nu_3 + \nu_{\text{ext}}$  spectra at 100°K for  $\text{NCO}^-$  isolated in various alkali halides, compared with the integrated density of states where available (see Refs. 13, 23, and 24).



TABLE II. Sharp features and lowest-energy broad bands in  $\nu_{\text{ext}}$  spectra of impurity ions in alkali halides. (See Table I, Ref. 5 for values obtained with other ions.) Energies quoted in  $\text{cm}^{-1}$ . Sharp features above and below the lowest optic-mode frequency of the host lattice are separated by a colon.

	Sharp features			Lowest-energy broad bands		
	NCO <sup>-</sup> at 100°K	NCS <sup>-</sup> at 40°K	CN <sup>-</sup> at 7°K	NCO <sup>-</sup> at 100°K	NCS <sup>-</sup> at 40°K	CN <sup>-</sup> at 7°K
NaCl	a	b	a	86	b	54
NaBr	117, 123, 127:a	b	110, 123:(156)	52	b	38
NaI	91, 105:a	89, 101:a	93:a	35	37	27
KCl	a	b	a	52	b	13.5
KBr	97, 100:168, 184	b	a	41	b	12
KI	78, 82:(133), 152	79, 83:163	83:a	31	26	12.5
RbCl	a	b	b	36	b	b
RbBr	a:141, 154	a:144, 184	b	31	24	b
RbI	a:115, 134	a:128, 148	b	24	18	b
CsCl	a	b	b	37	b	b
CsBr	a:119, 138	b	b	37	b	b
CsI	a:(81), 107	a:109, 135	b	40	29	b

<sup>a</sup> No features observable in spectra.  
<sup>b</sup> Spectra not yet investigated.

made to fit low-temperature neutron-scattering results for NaI,<sup>13</sup> KBr,<sup>13</sup> and KI,<sup>23</sup> and the others from the calculations of Karo and Hardy<sup>24</sup>).

Several general trends can be seen to exist in these spectra: (a) No sharp  $\nu_{\text{ext}}$  features are shown by the four chloride spectra. (b) In the bromides and iodides, the observed sharp features appear in the sodium salts only in-the-gap; in the potassium salts both in-the-gap and superoptic; and in the rubidium and caesium salts predominantly superoptic. (c) There is a tendency for the sharp features to occur as doublets, though the two components do not always seem to be of equal intensity. (d) The separation of the in-the-gap doublet seems to vary directly with the size of the gap. (e) The three cesium halides do not show the strong broad lowest-separation band which is to be seen in the other spectra. (f) Apart from the case of NaCl, which appears to show only the broad absorption at acoustic-band energies, all the spectra show a relatively strong feature at the extreme high-energy end of the optic band. This takes the form of the lower-energy component of the superoptic doublet in those cases where this doublet is clearly resolved. In those cases that show no superoptic structure it takes the form of the highest energy maximum in the  $\nu_{\text{ext}}$  spectrum, and in the cases of KI and CsI, lower-temperature spectra and high-pressure spectra (see below) suggest that this is still the low-energy component of the superoptic doublet which has just failed to rise clear of the optic-band modes in these two cases at zero pressure.

The fact that the chlorides show no sharp features will be returned to in the later discussion of the  $\nu_{\text{ext}}$  spectra shown by the cyanide ion, which is the only ion that we have so far used in this investigation which is lighter than the chloride ion.

The presence of in-the-gap modes in combination

with  $\nu_3(\text{NCO}^-)$  in the bromides and iodides seems to depend simply on whether or not a gap exists in the integrated density of states for the particular alkali halide. Thus we would feel justified in suggesting that there was no gap in RbBr, RbI, CsBr, or CsI, and that the calculations of Karo and Hardy<sup>24</sup> have put the gap in NaBr noticeably too low. For a superoptic mode to exist, the motion must be highly localized, and it therefore seems reasonable to suggest that the absence of these modes in NaBr and NaI is primarily due to the relative lightness of the nearest-neighbor sodium ions. These ions, being incapable of playing their part in such a vibration without having relatively large amplitudes, inevitably involve further ions, delocalize the motion, and thus hold down the frequency to within the optic band.

Following our assignment of the sharp bands in  $\nu_{\text{ext}}$  for NCO<sup>-</sup> in KBr as acoustic- and optic-torsional modes about two axes, which perpendicularly cut the N-C and C-O bonds, we would expect to see this general pattern repeated for NCO<sup>-</sup> in other lattices. Many of the spectra are seen to show evidence of similar in-gap and superoptic doublet structure, where it can reasonably be expected (i.e., in-gap if a gap exists, and superoptic if nearest neighbors are sufficiently massive). The two components of any given doublet of the described torsional origin would be expected to be similar in intensity. However, this does not always appear to be the case. The superoptic doublets in KI and CsI have been considered above. An extra component is to be seen in-the-gap in NaBr, and most of the imbalance between the components in-the-gap in NaI appears to be due to an underlying absorption presumably of similar origin to that of the extra band observed in NaBr. Thus, if the presence of extra in-gap or superoptic structure of an unspecified origin is accepted, then it does seem that the pattern of acoustic and optical-torsional-type doublets can be followed through these spectra.

<sup>23</sup> G. Dolling, R. A. Cowley, C. Schittenhelm, and I. M. Thorson, *Phys. Rev.* **147**, 577 (1966).

<sup>24</sup> A. M. Karo and J. R. Hardy, *Phys. Rev.* **129**, 2024 (1963).

The in-the-gap doublets, having grown out of the acoustic band, appear to have retained sufficient of their acoustic nature to find it very difficult to move up to an energy associated with optic-mode vibrations. Thus in KBr the in-gap doublet, having climbed clear of the acoustic band, finds itself almost immediately opposed and cramped into a very narrow energy band just below the optic modes. This results in the close spaced doublet observed in this case, which if the optic bands had started higher, might well have appeared as a much wider spaced doublet as is observed in KI and more particularly NaI.

The broad lowest-energy  $\nu_{\text{ext}}$  absorption which becomes increasingly evident as one goes from sodium to potassium to rubidium halides is not to be seen at all in the cesium halides, although a much sharper, weaker absorption, at higher energies, is found within the acoustic continuum. There is the obvious difference in structure between the cesium halides (CsCl type) and the other nine halides (NaCl type) to be considered, and also the orientation of the  $\text{NCO}^-$  ion within this structure.

Calculations of the energy of the system, as a function of  $\text{NCO}^-$  axis orientation within CsCl-type structures, suggest either a  $\langle 001 \rangle$  or a  $\langle 110 \rangle$  direction as the lowest-energy configuration, and rule out a  $\langle 111 \rangle$  orientation. Since  $\langle 110 \rangle$  would result in a splitting of  $\nu_2$  which is not observed, it seems fairly certain that the ion lies in a  $\langle 001 \rangle$  direction. Although the resultant  $C_{4v}$  symmetry

does not result in any rigid selection rules, it is worth considering the  $D_{4h}$  rules to see what trends to expect in the relative intensities of different types of absorption, as in the earlier discussion of  $C_{3v}\text{NCO}^-$  and  $D_{3h}\text{N}_3^-$  for the NaCl structure. As for the previously considered case, it is  $R_x$  and  $R_y$  which give the only active binary combinations with  $\nu_3$ , so there is no guide here as to the absence of the broad low-energy band in the CsCl structures. It may be that here again there is evidence of a directional property which cannot be adequately described by simple selection rules. These points will be considered again later when the NaCl to CsCl-type pressure induced phase changes are discussed.

The persistent appearance of a feature at the extreme high-energy limit of the optic band suggests that for some reason this feature is held located close to this point in the dispersion curves. This is used later when the pressure dependence of some of these spectra is used to obtain information about the pressure dependence of the host-lattice vibrations.

#### $\nu(\text{CN}^-) \pm \nu_{\text{ext}}$ SPECTRA FOR VARIOUS ALKALI HALIDES

Figure 8 shows the spectra recorded at 7°K for  $\text{CN}^-$  isolated the chlorides, bromides, and iodides of sodium and potassium. For the sodium halides these spectra have not changed radically in lowering the temperature from 90°K, and at this higher temperature the stronger

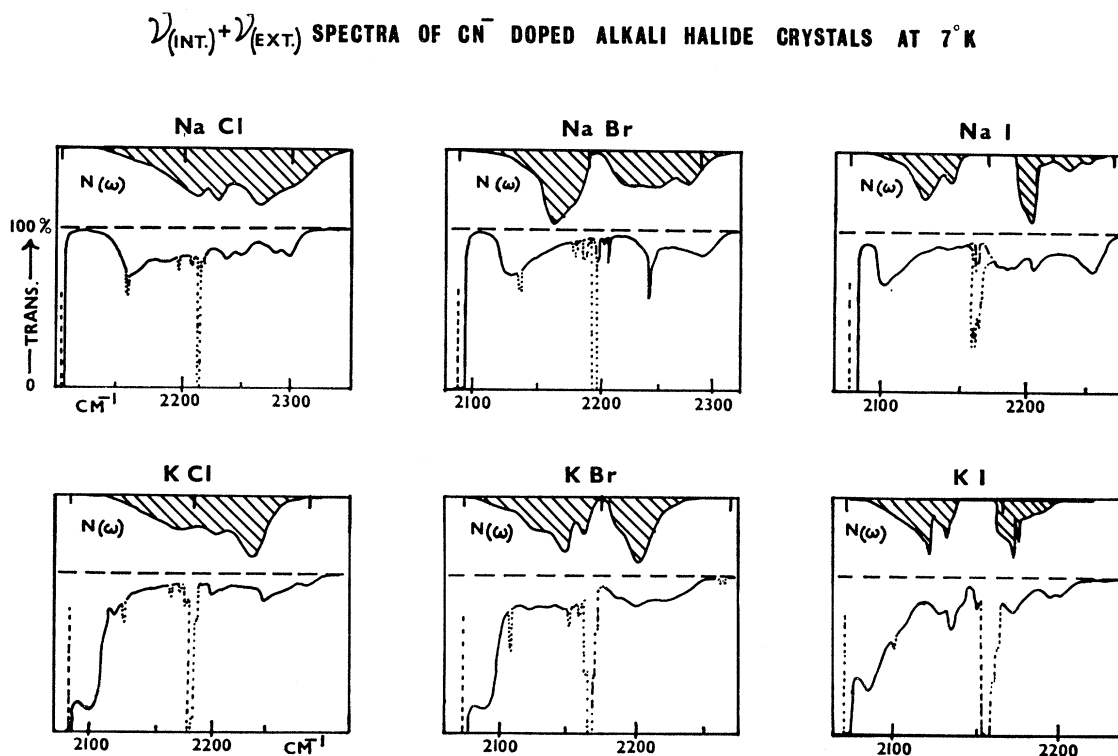


FIG. 8.  $\nu_{\text{int}} + \nu_{\text{ext}}$  spectra at 7°K for  $\text{CN}^-$  isolated in various alkali halides, compared with the integrated density of states for the pure crystals (see Refs. 13, 23, and 24).

features were all visible in the  $\nu_{\text{int}}-\nu_{\text{ext}}$  spectra, thus allowing us to be fairly sure about the features, if any, which are obscured by the  $\text{NCO}^-$  bands. Since the spectra for the potassium halides only began to show their true shape below 20°K, no such assistance from  $\nu_{\text{int}}-\nu_{\text{ext}}$  features is available for them.

Points of interest about these spectra may be listed as follows: (a) There are no strong sharp features in the chloride spectra. (b) There are no strong superoptic features in any of the spectra. (c) The smallest separation feature is only about  $12\frac{1}{2}$   $\text{cm}^{-1}$  above the main band for all three potassium halides, whereas it is seen at 27, 38, and 54  $\text{cm}^{-1}$ , respectively, in sodium iodide, bromide, and chloride.

The lightness of the impurity is seen not to be a dominant factor in determining the presence either of sharp features or strong superoptic structure in the  $\nu_{\text{ext}}$  spectra. Although the cyanide ion is lighter than the chloride ion which it replaces and the translational restoring forces are quite comparable to those acting on a host-lattice ion it is known<sup>17,19</sup> that the rotational restoring force is very small, particularly in the potassium halides. The absence of any in-the-gap or superoptic features which could be considered as directly analogous to the structure observed in the cyanate spectra appears to be consistent with the proposed torsional origin of the cyanate bands and the known tendency of the cyanide to perform hindered rotation in these alkali halides.

If the nature of the acoustic- and optic-torsional modes proposed for  $\text{NCO}^-$  is considered as a function of steadily decreasing torsional restoring force, then the acoustic torsion can be seen to go over into hindered rotation at a sufficiently low restoring couple. The fate of the optic-type mode is less obvious, but for still moderate restoring couple in the sodium halides, for example, it seems reasonable that such an oscillation could drop in frequency sufficient to find itself in the optic to acoustic gap. This may be the origin of some of the in-gap features observed for sodium bromide and iodide, but the possibility that they are essentially translational modes of the ion cannot be ruled out, especially in view of the extra in-gap structure shown by the spectra of  $\text{NCO}^-$  in these lattices.

Several further points which apply to individual spectra of Fig. 8 are worth mentioning.

In NaCl considerable absorption of a broad, but peaked, nature can be seen to extend well into the optic-band region, and this is to be contrasted with the  $\text{NCO}^-$  spectrum. The dominant factor here may well be the relative lightness of the  $\text{CN}^-$  ion.

Sharp in-gap structure is found for  $\text{CN}^-$  in NaBr at about the same separation as that observed for  $\text{NCO}^-$  and again suggests a wide gap at energies higher than those calculated by Karo and Hardy.<sup>24</sup> These in-gap bands were quite sharp at 90°K, at which temperature they could also be seen in  $\nu(\text{CN}^-)-\nu_{\text{ext}}$ . Contrasted with this, however, is the band at  $\nu(\text{CN}^-)+154$   $\text{cm}^{-1}$ , which

was still quite broad at 90°K, had sharpened somewhat by 25°K, but only attained the prominence shown in Fig. 8 below about 10°K. This band is discussed later in the section concerned with temperature effects.

Although the  $\text{NCO}^-$  band in NaI has always obscured  $\nu(\text{CN}^-)+93$   $\text{cm}^{-1}$  and several  $\text{cm}^{-1}$  on each side of this value, the band at this energy has been dotted-in, in Fig. 8, because it has been recorded repeatedly in  $\nu(\text{CN}^-)-\nu_{\text{ext}}$  at 90°K and frozen out at lower temperatures. By 7°K, its energy would probably have increased slightly, and it is interesting to compare this with the similar band observed directly in the far infrared by Lytle and Sievers.<sup>25</sup>

Evidence for a sharp line at  $\nu(\text{CN}^-)+82$   $\text{cm}^{-1}$  in KI is to be found in the spectrum shown in Fig. 8 and this may also be compared with the far-infrared work of Lytle and Sievers.<sup>25</sup>

The absorption, if any, shown by these  $\nu(\text{CN}^-)\pm\nu_{\text{ext}}$  spectra in-the-gap is particularly useful information, and it is most unfortunate that so much of this has been obscured by  $\nu_3(\text{NCO}^-)$  absorption. Our crystal-growing facilities are therefore being considerably extended to enable us to grow larger, more carefully controlled crystals with which to continue this investigation.

#### $\nu_{\text{ext}}$ SPECTRA FOUND IN COMBINATION WITH $\nu_3(\text{BO}_2^-)$ , $\nu_3(\text{N}_3^-)$ , AND $\nu_3(\text{NCS}^-)$

Other ions which may profitably be compared with  $\text{NCO}^-$  are  $\text{NCS}^-$ ,  $\text{BO}_2^-$ , and  $\text{N}_3^-$ .  $\text{BO}_2^-$  and  $\text{N}_3^-$ , because of their similarity with  $\text{NCO}^-$  in size, nuclear masses, internal force constants, etc., can be considered as limited extensions of the progression of  $\text{NCO}^-$  isotopic species discussed in detail earlier. Although these ions cannot be so easily incorporated into the alkali halides in the relatively high dopings used for the  $\text{NCO}^-$  samples, the spectra so far obtained have been strong enough to show two points of interest. (i) The in-gap and superoptic doublets which have been shown to be characteristic of the  $\text{NCO}^-$  spectra have always been replaced by single lines in the  $\text{BO}_2^-$  and  $\text{N}_3^-$  spectra. (ii) Within the limits set by the reduced absorption intensity, no broad features have been identified in these spectra. These two points should be considered together with the introductory comments on the type of motion expected to combine with  $\nu_3$  of these ions under the prevailing  $D_{3d}$  selection rules. Added weight is then given to the proposal that the sharp features in these spectra, and in the spectra combined with  $\nu_3(\text{NCO}^-)$ , represent essentially torsional motion of these ions, and this suggests that translational impurity motion should be associated with the broader features in these cases.

$\text{NCS}^-$  could be considered as a distant extension of the progression of  $\text{NCO}^-$  isotopic species, but here the extreme asymmetry of the ion might be expected to

<sup>25</sup> C. D. Lytle and A. J. Sievers, Bull. Am. Phys. Soc. **10**, 616 (1965).

change the nature of the doublets and also to increase the relative intensity of translational-type modes in binary combination with  $\nu_3$ . Note that the infrared activity of the various internal modes of an impurity ion gives an indication of the probable degree of selection operating in combinations of internal with external modes; e.g., for  $\text{NCO}^-$ ,  $2\nu_3$  is unobservably weak [even in the strongest samples so far used, where  $\nu_3$  of double isotopic species such as  $(\text{N}^{15}\text{CO}^{18})^-$  in natural abundance of about 0.0007% can be easily seen],  $\nu_1$  is about 30 times weaker than  $\nu_3$ ,  $\nu_3 + \nu_2$  is very weak, etc. This pattern shows a clear tendency towards the  $D$  symmetry rules, by which this slightly asymmetric ion cannot really be governed. The  $2\nu_3$  for  $\text{NCS}^-$  is, however, clearly visible even in samples which contain only moderate dopings.

The increased size of this ion does, however, limit its use, for although it can be introduced in low concentrations into all the various alkali-halide crystals such that its internal modes can be easily recorded,<sup>26</sup> it is difficult to obtain sufficient concentration to observe the much weaker  $\nu_{\text{int}} \pm \nu_{\text{ext}}$  spectra. Thus only in the four iodides have we obtained good external-mode features in

combination with  $\nu_3$  of this ion. Figure 9 shows the four spectra for sample temperatures of about 40°K. This lower temperature was required to bring the spectra to a degree of sharpness comparable with that shown by the  $\text{NCO}^-$  spectra at 100°K. As with our heavily doped cyanide crystals, these spectra also show the  $\nu_3(\text{NCO}^-)$  absorption, which is again at an unfortunate spacing from the  $\nu_3(\text{NCS}^-)$ . However, these spectra are all sufficiently sharp at 100°K for the  $\nu_{\text{int}} - \nu_{\text{ext}}$  spectra to show unambiguously what features are being obscured, and these have been "dotted-in" in Fig. 9.

The sodium-, rubidium-, and cesium-iodide spectra show a shifting of the emphasis from the sharp doublets towards the low-energy broad feature when compared with the corresponding  $\text{NCO}^-$  spectra (Fig. 7). For  $\text{NCS}^-$  in both potassium and cesium iodide, the spectra look qualitatively quite different from the equivalent  $\text{NCO}^-$  spectra. We suggest the possibility that in these two crystals the different impurities align in different orientations. There is good evidence to support this in the case of CsI, for in all the cesium halides different internal-mode frequencies can be obtained by varying the conditions under which the doped crystals are

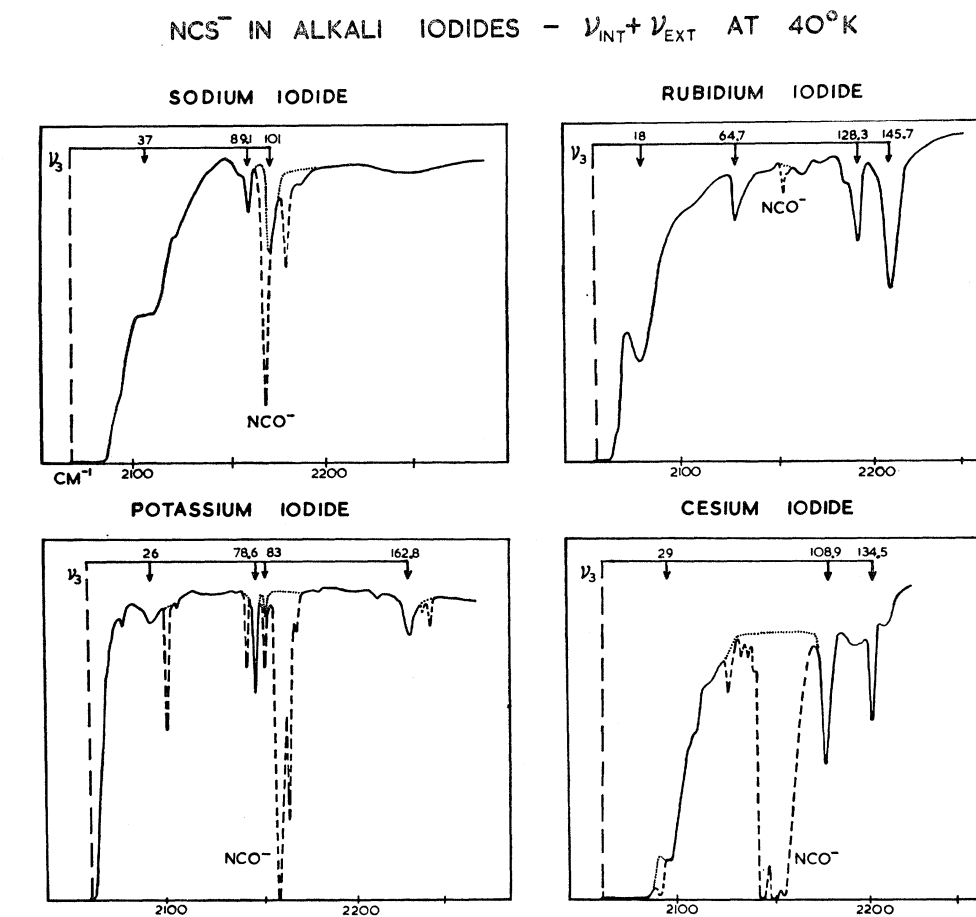


FIG. 9.  $\nu_3 + \nu_{\text{ext}}$  spectra at 40°K for  $\text{NCS}^-$  isolated in alkali iodides. Features due to  $\text{NCO}^-$  are shown dashed.

<sup>26</sup> M. A. Cundill and W. F. Sherman (to be published).

grown. (See Ref. 26 for more detail on this point.) The internal-mode frequency for the crystal used to obtain the spectrum in Fig. 9 is such as to suggest an orientation of the  $\text{NCS}^-$  different to that of the  $\text{NCO}^-$  which gave the spectrum of Fig. 7. So far we have not grown a high-concentration  $\text{NCS}^-$ -doped CsI crystal with the alternative orientation.

The in-gap doublets shown by the NaI and KI spectra occur at energies close to those observed in the  $\text{NCO}^-$  spectra, re-emphasizing the extent to which the host lattice dictates these frequencies. The more localized superoptic frequencies show a greater disparity between the  $\text{NCS}^-$  and  $\text{NCO}^-$  numbers, as might be expected for bands which are more dependent on impurity mass and localized-force constants than on host-lattice dispersion curves.

#### $\nu_{\text{ext}}$ IN COMBINATION WITH DIFFERENT INTERNAL MODES

The ease with which good  $\text{NCO}^-$ -doped crystals can be produced has led to this ion's being used only in this part of the investigation. Figure 7 showed  $\nu_{\text{ext}}$  as observed in combination with  $\nu_3(\text{NCO}^-)$ . The other internal modes which are strong enough to give a reasonable chance of observing  $\nu_{\text{int}} \pm \nu_{\text{ext}}$  spectra are  $\nu_2$  (the doubly degenerate bending mode at about  $630 \text{ cm}^{-1}$ ) and the  $\nu_1, 2\nu_2$  fermi doublet (at about  $1200$  and  $1300 \text{ cm}^{-1}$ , with  $\nu_1$  being the more symmetric of the two stretching modes). All these three bands are down by a factor of about 30 in intensity compared with the  $\nu_3$  mode, and the external modes in combination with them are down by about the same factor when compared with  $\nu_3$  sidebands. Thus even the strongest samples so far used have only shown the most intense features in  $\nu_{\text{ext}}$  in combination with  $\nu_2, \nu_1$ , and  $2\nu_2$ . Although the first, and strongest, sample (1 cm of RbBr having about 1.5%  $\text{NCO}^-$  for  $\text{Br}^-$  replacement) that we used to investigate these other bands appeared to show extra structure in combination with  $\nu_2$ , our subsequent spectra have shown these bands to have been due to other impurities.

In all cases so far investigated, the strongest lattice sidebands found on  $\nu_3$  have also been found on all three of the other bands ( $\nu_2, \nu_1$ , and  $2\nu_2$ ) at separations which were the same within the experimental reliabilities. Thus, so far we have failed to find evidence from this part of the investigation to support the idea of directional selection of  $\nu_{\text{ext}}$  modes which show strong binary combination with  $\nu_{\text{int}}$ . This is not to say that the idea must be rejected, since it was only postulated to apply to the broader, delocalized structure which has yet to be recorded in these other regions. It is hoped to continue this part of the investigation with larger, more heavily doped crystals, since only a factor of about 5 in sample absorption is estimated to be required before a positive assessment of the more intense broad features could be made.

#### TEMPERATURE EFFECTS

All the  $\nu_{\text{int}} \pm \nu_{\text{ext}}$  spectra were recorded at 300 and  $100^\circ\text{K}$ , many were also recorded at about  $30^\circ\text{K}$ , using a Norelco-Cryogem sample cooler, and some were studied over the whole temperature range from  $7$ – $450^\circ\text{K}$ . The sharp features on each side of the internal mode always appeared, within the experimental accuracy, to have intensities relative to one another which were simply determined by the thermal populations of the respective lower levels. Superoptic features were found to broaden and decrease in separation from  $\nu_{\text{int}}$  more rapidly with increasing temperature than in-gap features (see, e.g., Fig. 10). Broad features, though less easy to measure, seemed to show intensity changes over and above those associated with binary combinations having thermally controlled populations in their lower levels. An example of such behavior is the lowest-separation broad band in  $\nu_3(\text{NCO}^-)$  spectra, where at lower temperatures there appeared a definite reduction of intensity in the summation band feature. It would seem that the presence of other phonons, playing an energetically neutral part, increase the transition probability of this combination.

Two particular temperature-induced changes seem to warrant individual comment. Firstly, the relatively broad band observed for  $\text{CN}^-$  in NaBr at  $90^\circ\text{K}$  at  $154 \text{ cm}^{-1}$ . At temperatures below  $25^\circ\text{K}$  this band sharpens quite markedly, until at  $7^\circ\text{K}$  it dominates the  $\nu_{\text{ext}}$  spectrum and is seen in Fig. 8 to be a sharp band situated almost in the center of the optic band as calculated by Karo and Hardy.<sup>24</sup> This is the only absorption clearly within the optic band of the host lattice that has been found to show this dramatic sharpening.

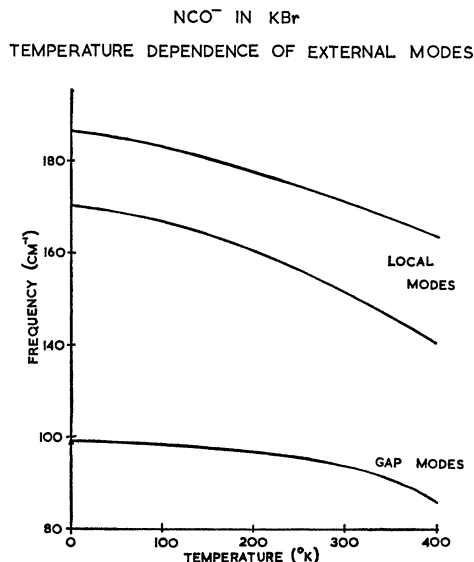


FIG. 10. Temperature dependence of the frequencies of the sharp external-mode features found in combination with  $\nu_3(\text{NCO}^-)$  in KBr.

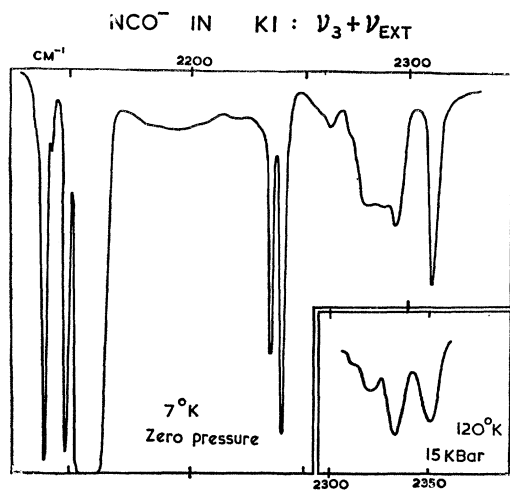


FIG. 11.  $\nu_3 + \nu_{\text{ext}}$  spectrum of  $\text{NCO}^-$  in KI at  $7^\circ\text{K}$  and zero pressure with insert showing the superoptic doublet region at  $120^\circ\text{K}$  and 15 kbar pressure. The strength of the main  $\nu_3$  line at  $2157\text{ cm}^{-1}$  can be judged from the intensities of the  $\text{O}^{18}$  and  $\text{N}^{15}$  isotopic species seen to slightly lower frequencies. Note the reduced intensity of the low-energy broad external-mode band when compared with the  $100^\circ\text{K}$  spectrum of Fig. 7 and the more clearly resolved lower component of the superoptic doublet.

The  $\langle 001 \rangle$  orientation of the ion is believed to be significant, as is the fact that this energy coincides with a clearly marked minimum in the  $\nu_{\text{ext}}$  spectrum found in combination with  $\nu_3$  of the  $\langle 111 \rangle$ -oriented  $\text{NCO}^-$  ion. Secondly, the effect of lowering the temperature of  $\text{KI} + \text{NCO}^-$  to  $7^\circ\text{K}$  is shown in Fig. 11. If this spectrum is compared with the  $90^\circ\text{K}$  spectrum of Fig. 7, the relative intensity of the lowest-separation broad band is seen to have decreased (as was found generally to be the case; see above), but of particular interest is the superoptic region. Here the  $152\text{-cm}^{-1}$  band has sharpened further, and moved out to  $155\text{ cm}^{-1}$ , and the  $133\text{-cm}^{-1}$  band has moved out to  $137\text{ cm}^{-1}$  and can be seen to be sharper and almost resolved from the general optic-band absorption. The description of these two bands as the optic-torsional doublet can be seen to look much more reasonable in this very-low-temperature spectrum. Also included as an inset in Fig. 11 is the 15-bar  $120^\circ\text{K}$  spectrum, which shows the band originally at  $133\text{ cm}^{-1}$  even more clearly resolved from the general optic-band absorption.

### PRESSURE EFFECTS

The effects of high pressures on absorption bands which show lattice sideband structure have been investigated, using a modified Drickamer type<sup>27</sup> of high-pressure optical cell working up to 50 kbar at temperatures in the range  $90\text{--}500^\circ\text{K}$ .<sup>23</sup> Some of the spectra recently recorded have been obtained, using later modifications to the high-pressure cell design in

<sup>27</sup> H. G. Drickamer, R. A. Fitch, and T. E. Shykhov, *J. Opt. Soc. Am.* **47**, 1015 (1957).

<sup>28</sup> W. F. Sherman, *J. Sci. Instr.* **43**, 462 (1966).

which samples up to  $\frac{1}{2}$  in. along the radiation path may be investigated at about  $120^\circ\text{K}$  up to pressures above 40 kbar. All spectra included an internal pressure calibrant<sup>28</sup> which allowed sample pressures to be quoted to within a fraction of a kbar with respect to our primary pressure calibrant, the shift of  $\nu_3(\text{NCO}^-)$  in NaCl as quoted by Drickamer *et al.*<sup>27</sup>

### PRESSURE-INDUCED PHASE CHANGES

Perhaps the most interesting change to observe as the pressure is increased is the change that takes place when a potassium or rubidium halide changes from its low-pressure NaCl-type structure to its high-pressure CsCl-type structure. Even at the relatively great impurity-ion concentrations ( $\approx 1\%$ ) required for the observation of lattice-sideband spectra, no meaningful changes are observed in the pressures at which the phase changes take place, but the onset of the change becomes increasingly sluggish as the doping increases.

Figure 12 shows the  $\nu_3 \pm \nu_{\text{ext}}$  spectrum for  $\text{NCO}^-$  isolated in RbBr at two different pressures in the low-pressure phase and two different pressures in the high-pressure phase. The lowest-pressure spectrum is somewhat inferior to that shown in Fig. 7, due partly to the temperature of the high-pressure cell being slightly above that obtainable with a standard cold cell, and partly to the disrupting effect of pressing the sample into the pressure cell. The center frequency of the main band is indicated at each pressure by a vertical dashed line.

Using the  $\text{C}^{13}$  isotopic line as a guide to the effect of pressure on the internal mode, the phase change can be seen to have caused a noticeable increase in frequency and also to have produced an unfortunate pair of satellite lines on the low-energy side of the band. It is

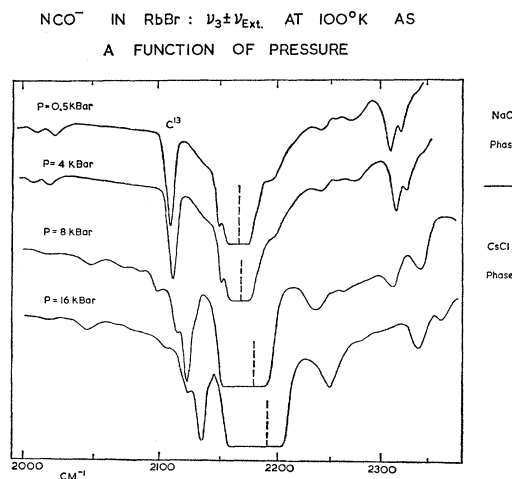


FIG. 12. Effect of pressure at  $100^\circ\text{K}$  on the  $\nu_3 \pm \nu_{\text{ext}}$  spectrum of  $\text{NCO}^-$  in RbBr. The center frequency of the main line is indicated by a vertical dashed line and its intensity can be gauged from that of the 1.1% natural abundance  $\text{NC}^{13}\text{O}^-$  line.

these two satellite bands, increased by the relative abundance ratio of about 90, which give the main band its much increased width in the upper phase. However, the high-energy side of the line is fairly sharp, and this has allowed the  $\nu_3 + \nu_{\text{ext}}$  spectrum to be seen reasonably clearly to within about  $20 \text{ cm}^{-1}$  of the main line.

On going through the phase change, the prominent low-separation band peaking at about  $\nu_3 + 31 \text{ cm}^{-1}$  disappears and is replaced by a less intense though more clearly resolved band at about  $\nu_3 + 55 \text{ cm}^{-1}$ . The superoptic doublet becomes much wider spaced in the upper phase and is found closer to the main line. These changes are probably seen more clearly in Fig. 13, where the three most prominent  $\nu_{\text{ext}}$  energies in each phase are plotted as a function of pressure.

Since, as discussed earlier, the lower component of the superoptic doublet is always found close to the maximum optic-mode frequency of the pure lattice, Figs. 12 and 13 show that this maximum optic-mode frequency decreases as RbBr is compressed through its NaCl to CsCl structure phase change. The interpretation of the low-separation absorption is less clear, but the marked increase ( $31\text{--}55 \text{ cm}^{-1}$ ) of its maximum suggests a marked increase in the relevant acoustic-lattice modes. Although this would be the expected result of the increased density of the high-pressure phase, the initial negative slope of the  $\nu_3 + 31 \text{ cm}^{-1}$  line suggests that such an explanation is oversimplified.<sup>29-31</sup>

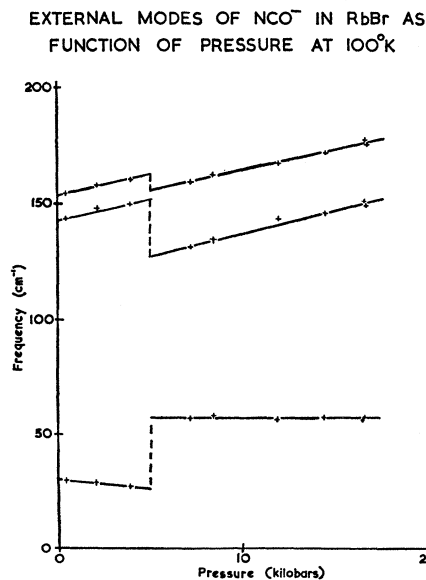


FIG. 13. Pressure dependence of the frequencies of the prominent features in the lattice-sideband structure to  $\nu_3(\text{NCO}^-)$  isolated in RbBr at  $100^\circ\text{K}$  (cf. Fig. 12).

<sup>29</sup> The difference between these bands and the monatomic-impurity low-energy resonance bands discussed by Benedek and Nardelli (Ref. 11) must again be underlined here. The general differences were discussed earlier in the section on  $\text{CN}^-$  in KBr, but the difference in behavior under pressure should be noted at this point. (i) In the low-pressure phase, the band shows a definite decrease in frequency as the pressure is raised, which is the

#### EXTERNAL MODES OF $\text{NCO}^-$ IN $\text{KBr}$ AT $140^\circ\text{K}$

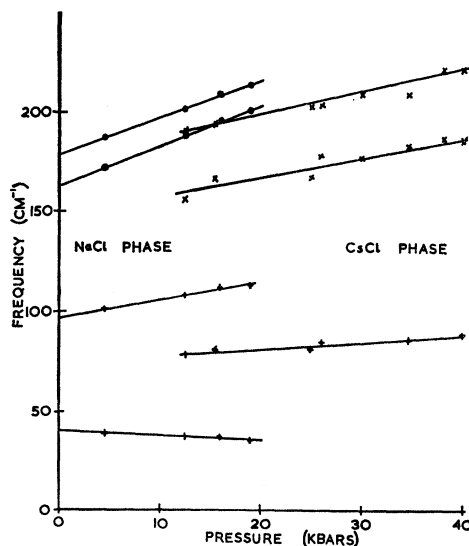


FIG. 14. Pressure dependence of the frequencies of the prominent features in the lattice-sideband structure on  $\nu_3(\text{NCO}^-)$  isolated in KBr at  $140^\circ\text{K}$  (cf. Fig. 2). The in-gap doublet (NaCl phase) had to be plotted as a single line on this scale, although the two components could still be distinguished up to the phase change in spite of a slight broadening of the spectral features under pressure.

Since no sharp features appear near the center of the  $\nu_{\text{ext}}$  spectrum of the upper phase, it seems fair to conclude that there is no gap in the integrated phonon density of states of the CsCl-structured RbBr.

Figure 14 shows the pressure dependence of the most prominent  $\nu_{\text{ext}}$  features in the  $\nu_3 \pm \nu_{\text{ext}}$  spectrum of  $\text{NCO}^-$  in KBr. All the effects noted above for RbBr are seen again in this case. The strong sharp in-gap doublet, plotted as a single line in Fig. 14, has no analogous feature in the CsCl-structured high-pressure phase, suggesting that here again there is no gap in the integrated phonon density of states of the high-pressure phase.

The  $\nu_3 \pm \nu_{\text{ext}}$  spectra for  $\text{NCO}^-$  in both RbI and KI have also been recorded as a function of pressure at low temperature. In these two cases also the same general trends were observed at the phase change, i.e., (i) a lowering in energy and widening of separation of the superoptic doublet, (ii) the replacement of the broad

opposite behavior to that of the monatomic-impurity resonance mode. (ii) In the upper phase the band appears at a much higher energy, which takes it very much closer to the reststrahlen frequency which has dropped in energy during the phase change (see above and Refs. 30 and 31), and yet it is a much sharper band in marked contrast to the findings of Benedek and Nardelli (Ref. 11) for the monatomic resonance bands which broaden very rapidly when pushed under pressure towards the reststrahlen frequency.

<sup>30</sup> S. S. Mitra, J. N. Plendl, and L. C. Mansur, in Proceedings of the Ninth European Congress on Molecular Spectroscopy, Madrid, 1967 (unpublished). See also Phys. Rev. Letters **18**, 455 (1967).

<sup>31</sup> W. G. Fateley, N. T. McDevitt, and R. E. Witkowski, in Proceedings of the Ninth European Congress on Molecular Spectroscopy, Madrid, 1967 (unpublished).

very-low-energy absorption by a sharper feature at almost twice the energy, and (iii) the absence of any in-gap structure in the high-pressure phase.

Before leaving the topic of effects due to the NaCl-type to CsCl-type phase change, some consideration should be given to the low-separation band in the NaCl structure, which decreases in energy as the pressure is raised. This decrease, in marked contrast to all other bands, even the feature which appears to take its place in the CsCl structure, may be indicating a tendency towards instability at the phase change, but it must be emphasized that this band had only decreased by about 15% in each case (see, e.g., Figs. 13 and 14) before the phase change occurred. In general, the steady shifts which the various bands show as a single phase is compressed indicate the changes in the relevant force constants with pressure. Although for any one particular localized mode this information is of fairly limited interest, in those cases where the band can reasonably be associated with a point in the dispersion curve of the pure host lattice these shifts carry information about the anharmonicity of the host-lattice forces, and this is a topic of more general concern.

#### PRESSURE DEPENDENCE OF IN-GAP LOCALIZED MODE

KBr has such a narrow gap that in following the sharp in-gap modes one is effectively monitoring this parameter of the host crystal. Figure 15 shows the pressure dependence of the in-gap modes observed in the  $\nu_3 + \nu_{\text{ext}}$  spectra of  $\text{NCO}^-$  and  $\text{N}_3^-$  isolated in KBr. As expected, the results for the two different ions are virtually identical. The continued presence of sharp

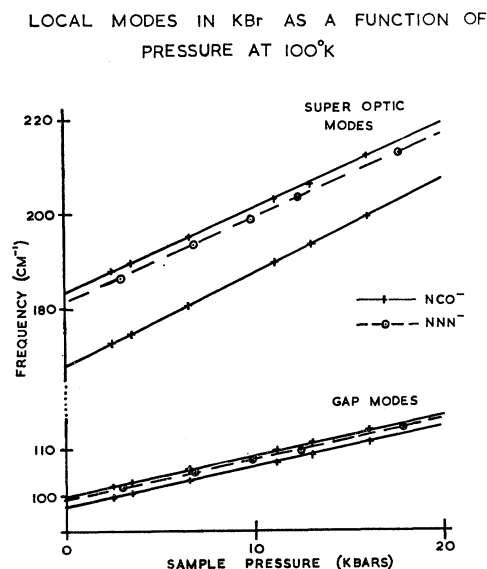


FIG. 15. Comparison of the pressure dependence of the local-mode frequencies of  $\text{NCO}^-$  and  $\text{N}_3^-$  in the low-pressure phase of KBr at 100°K.

bands shows that the gap still exists at elevated pressures, and the absence of noticeable divergence of the two  $\text{NCO}^-$  lines suggests that the gap does not widen appreciably. Thus it is suggested that both the LA and TO at  $(\frac{1}{2} \frac{1}{2} \frac{1}{2})$  (the modes limiting the gap; see Ref. 13) increase at the rate shown by the gap modes in Fig. 15. The TO at the band center is expected to rise slightly faster than this.<sup>32</sup>

Not all the external-mode features show the straight-line-frequency-versus-pressure type of graph illustrated in Figs. 13–15. The 105- $\text{cm}^{-1}$  line of the  $\text{NCO}^-$  in NaI external-mode spectrum has a very curved appearance, as shown in Fig. 16. At pressures above about 12 kbar this line is seen to be straight to within the experimental accuracy and this portion of the graph extrapolates back to an intercept of about 111  $\text{cm}^{-1}$ , which is fairly close to the lowest-energy optic mode ( $\text{TO}(\frac{1}{2} \frac{1}{2} \frac{1}{2}) \approx 117$ ).<sup>33</sup> The first impression that this gives is that the localized acoustic-torsional mode of the  $\text{NCO}^-$  isolated in an oversize iodide site, being very sensitive to pressure, rises rapidly until it meets the bottom of the optic band, whereafter it is constrained to move more slowly with the main lattice modes. However, the band center TO frequency has been calculated to fair accuracy at zero pressure, using the rigid-ion model,<sup>33–35</sup>

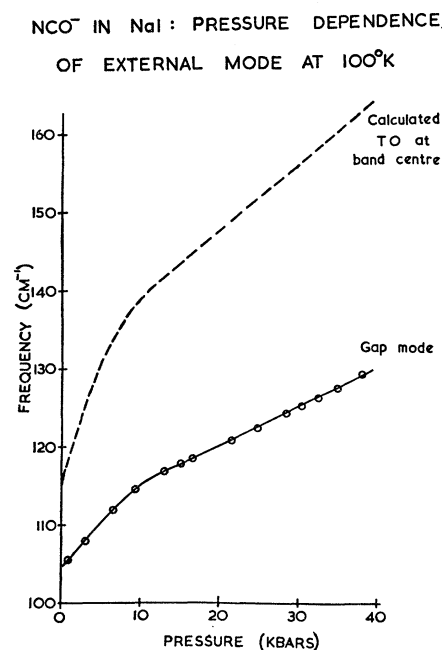


FIG. 16. Observed pressure dependence of the strongest in-gap mode for  $\text{NCO}^-$  in NaI (cf. Fig. 7) compared with the calculated change in the TO band-center frequency.

<sup>32</sup> The temperature dependence of the in-gap modes (Fig. 10) is very close to that of the TO at the band center (see, e.g., Ref. 13).

<sup>33</sup> B. G. Dick and A. W. Overhauser, *Phys. Rev.* **112**, 90 (1958).

<sup>34</sup> M. Born and K. Huang, *Dynamic Theory of Crystal Lattices* (Oxford University Press, Oxford, England, 1954).

<sup>35</sup> B. Szigeti, *Trans. Faraday Soc.* **45**, 155 (1945).



where

$$\bar{M}\omega_0^2 = A - \frac{\frac{4}{3}\pi N s^2 e^2}{1 - \frac{4}{3}\pi N(\alpha_+ + \alpha_-)}. \quad (1)$$

Here  $\bar{M}$  is the reduced mass of the positive and negative ions,  $N$  is the number of ion pairs per unit volume,  $se$  is the effective ionic charge, and  $A$  is a force constant, which is given by  $6R_0/K$  for a NaCl-type structure at zero pressure, where  $R_0$  is the nearest-neighbor distance and  $K$  is the compressibility. At nonzero pressures, a second term involving pressure  $P$  is needed, and  $A$  is modified to  $6R_0/K - 8RP$ .

If the effective charge and the ionic polarizabilities can be regarded as constant, then the band center TO frequency can be calculated using experimental values of compressibility as the sole experimental parameter which varies as a function of pressure. Experimental results on the change of dielectric constant with pressure seem to indicate that changes in  $\alpha_+$  and  $\alpha_-$  could effect the TO frequency by only 2 or 3%. The variation of effective charge  $se$  with pressure is considered later and is also found to be a relatively small effect. Since the TO at the band center is very close to the lowest optic-mode energy for NaI, the band center TO frequency can be taken as a good indicator of this energy. Using a very carefully drawn curve through Bridgman's<sup>36</sup> data for NaI, the compressibility (at 300°K) was obtained at various pressures and hence to TO frequency at these pressures calculated. These calculated TO values joined by a dotted line are also shown in Fig. 16, and it can be seen that the unusual shape of the in-gap external mode frequency versus pressure curve is to be found further emphasized in these calculated TO-versus-pressure curves. The reliability of the calculation is, of course, suspect, since it is so very sensitive to slight changes in slope of the  $\Delta V/V$ -versus-pressure graph which is undoubtedly different at the lower temperature which should have been used if the data had been available. However, far from catching up to the optic band and then being restrained by it, the external-mode frequency appears qualitatively to follow the TO mode, although showing a rate of change less than that of the pure lattice mode.

#### PRESSURE DEPENDENCE OF SUPEROPTIC LOCALIZED MODES

As mentioned earlier, there always seems to be a feature in all the  $\text{NCO}^- \nu_3 \pm \nu_{\text{ext}}$  spectra which corresponds to the top of the optic band of the pure lattice. It therefore seems fairly safe to assume that this feature moves under pressure in such a way as to monitor the top of the optic band. Unfortunately, from the point of view of utilizing this fact, calculated values of LO frequencies are unreliable when simple models are used. One can, however, approach this mode via the TO and

the LST<sup>37</sup> relationship  $(\epsilon_0/\epsilon_\infty)^{1/2} = \nu_{\text{TO}}/\nu_{\text{LO}}$ . Note that this expression was shown to hold at zero pressure by Woods *et al.*<sup>13</sup> within the accuracy of the neutron-scattering data.

If the data of Gibbs and Jarman<sup>38</sup> and of Burstein and Smith<sup>39</sup> on the pressure dependence of  $\epsilon_0$  and  $\epsilon_\infty$  of KBr are used, then the LO pressure dependence can be changed via the LST relationship to the TO pressure dependence. A rigid-ion model can then be used to evaluate the band center TO frequency and Szigeti's<sup>35,40</sup> relationships used to explain any slight disparity between observed and calculated values. The most convenient expression to use is

$$\left(\frac{e^*}{e}\right)^2 = S^2 = \frac{9\bar{M}\omega_0^2(\epsilon_0 - \epsilon_\infty)}{4\pi N e^2(\epsilon_\infty + 2)^2}, \quad (2)$$

where the notation is the same as that used for Eq. (1). Since the dielectric-constant data are limited to zero-pressure values of the rates of change of  $\epsilon_0$  and  $\epsilon_\infty$  with pressure, Eq. (2) was differentiated with respect to pressure and a value obtained for the rate of change of  $S$  with pressure. A value of  $(\partial S/\partial p)_0 = -0.9 \times 10^{-3}$  kbar<sup>-1</sup> was obtained.

Both the size and the sign of the above result are of interest. The very small numerical value is to be expected, since the effective charge is found to vary very little over a wide range of different alkali halides,<sup>40</sup> and might therefore be predicted to change only slowly in a given alkali halide as a function of pressure. The negative sign of the pressure coefficient is consistent with Szigeti's<sup>40</sup> explanation of the significance of the effective charge. Since the effective charge is found to be less than the electronic-charge, Szigeti concludes that as an ion approaches its nearest neighbor, there is a reduction in the total electron density along the line of centers of the two ions. This indicates the dominance of repulsive forces in determining local distortions of the electron cloud. Under pressure the ions are forced closer together, the short-range repulsive term becomes still more dominant, and  $(\partial S/\partial p)$  would be expected to be negative.

The small negative value obtained for  $(\partial S/\partial p)_0$  does suggest that the starting assumption that the 167-cm<sup>-1</sup> band in the  $\nu_{\text{ext}}$  spectrum was monitoring the LO frequency was reasonably justified, and it may therefore prove to be worthwhile using a more complex model for the alkali halide when assessing the significance of these shifts with pressure. However, as can be seen from Fig. 15, the 167-cm<sup>-1</sup> band moves very rapidly with pressure (and temperature; see Fig. 10), which is contrary to the predicted behavior of the LO band-center frequency.<sup>30</sup> It may be, therefore, that this

<sup>37</sup> R. H. Lyddane, R. G. Sachs, and E. Teller, *Phys. Rev.* **59**, 673 (1941).

<sup>38</sup> D. F. Gibbs and M. Jarman, *Phil. Mag.* **7**, 663 (1962).

<sup>39</sup> E. Burstein and P. L. Smith, *Phys. Rev.* **74**, 229 (1948).

<sup>40</sup> B. Szigeti, *Proc. Roy. Soc. (London)* **A204**, 51 (1950).

<sup>36</sup> P. W. Bridgman, *Proc. Am. Acad. Arts Sci.* **76**, 1 (1945).

feature has moved under pressure away from the special position that it occupied, at the very top edge of the optic band, at zero pressure. See also Fig. 11, which seems to indicate that the lower component of the "superoptic" doublet for  $\text{NCO}^-$  in KI moves with respect to the optic band when the crystal is compressed.

Bridgman's<sup>36</sup> data for KBr were also used with Eq. (1) to calculate TO frequencies for KBr similar to those described for NaI earlier. There was a very slight but possibly significant difference when the  $167\text{-cm}^{-1}$  band's pressure dependence was compared, via the Szigeti relationships, with these calculations, rather than by the direct use of Eq. (2). This difference could be expressed as a very slight pressure dependence of Szigeti's<sup>40</sup>  $K^*/K$  value.

The absence of pressure-dependent dielectric-constant data for other alkali halides makes the above type of analysis impossible for the superoptic features of ions in other alkali halides. However, Figs. 13-15 show some of the shifts that we have observed for superoptic external-mode features for  $\text{NCO}^-$  in alkali halides. All the spectra shown in Fig. 7 to possess superoptic features have also been investigated and show the same general trends. Only in one case,  $\text{NCO}^-$  in CsI, has a noticeably nonlinear frequency shift rate with pressure been observed.

#### EFFECTS OF PRESSURE ON $\nu_{\text{C-H stretch}} \pm \nu_{\text{ext}}$ FOR $\text{CHI}_3$

All the pressure effects discussed above have been concerned with doped alkali halides, although, as was pointed out in the Introduction, the  $\nu_{\text{int}} \pm \nu_{\text{ext}}$  type of spectrum is quite commonly found for a wide range of different systems. All such spectra could reasonably be investigated as a function of pressure, and information obtained about the respective crystal forces. As an example of a crystal containing binding forces very different from those of the alkali halides, we have investigated  $\text{CHI}_3$ .

Figure 17 shows a zero-pressure spectrum of the C-H stretching region of an iodoform crystal looking along the direction containing the C-H bonds, and shows how the broad wings were observed to expand as the pressure was increased at  $100^\circ\text{K}$ . The spectrum deteriorated as the pressure was increased, presumably due to a progressively worsening alignment of the C-H bonds, but the wings were still fairly well defined up to 25 kbar, by which pressure both the upper and lower defining energies had increased by about 50%. This very rapid rise might be expected for molecular crystals with small initial binding forces.

#### CONCLUSIONS

A considerable amount of theoretical work has been published recently on the vibration of impurities within

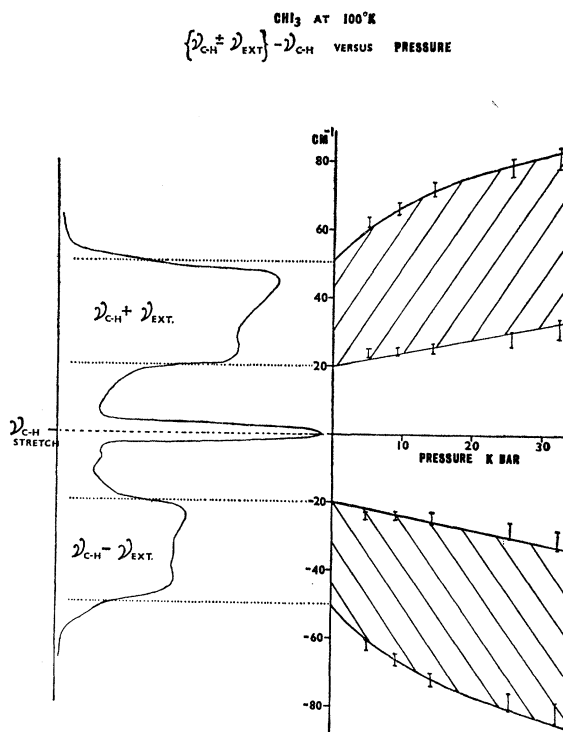


FIG. 17. Effect of pressure on the lattice sidebands on the C-H stretching vibration of iodoform at  $100^\circ\text{K}$ .

crystals (see, e.g., Refs. 11, 41-44), often with a good degree of agreement with experimental work on point defects. The extension of the theoretical work to include molecular impurities has been less convincing, however. Part of the purpose of this paper has been to underline two aspects of the molecular-impurity problem which seem to receive too little attention in the theoretical studies. These are (i) torsional motion of the impurity, and (ii) a directional selection of the modes which appear in strong binary combination with an essentially internal, vibrational (or electronic) transition of the impurity. The different  $\nu_{\text{ext}}$  spectra shown by  $\langle 111 \rangle$ -oriented  $\text{NCO}^-$  and  $\langle 001 \rangle$ -oriented  $\text{CN}^-$  in the sodium and potassium halides show conclusively that these spectra cannot possibly be simply monitoring the total integrated density of states of the host lattice. Some conclusions about the host-lattice dispersion curves can be drawn, however, and these are summarized below.

#### External Modes within the Acoustic Band of the Host Lattice

Broad, poorly defined absorption has usually been found in the external-mode spectra at energies covered

<sup>41</sup> A. A. Maradudin, *Solid State Phys.* **19**, 1 (1966).

<sup>42</sup> P. G. Dawber and R. J. Elliott, *Proc. Roy. Soc. (London)* **A273**, 222 (1963).

<sup>43</sup> R. W. H. Stevenson, *Phonons* (Oliver and Boyd, Edinburgh, 1966).

<sup>44</sup> *Proceedings of the International Conference of Lattice Dynamics, Copenhagen, 1963*, edited by R. F. Wallis (Pergamon Press, Inc., New York, 1965).

by the acoustic band of the host lattice. This absorption appears to bear some relation to the "structures due to host-lattice dynamics," which are predicted by Benedek and Nardelli,<sup>11</sup> but is quite different from the low-frequency resonance mode which is the subject of most of Ref. 11. We only feel justified in describing these features as a selection of the delocalized acoustic-type modes of the impurity-distorted lattice. The *decrease* of the frequency of the lowest energy band with increasing pressure as potassium and rubidium halides approach their phase change is an indication of a tendency towards instability of the relevant modes.

#### In-Gap Localized Modes

For NaCl, KCl, RbCl, RbBr, RbI, CsCl, CsBr, and CsI, no gap modes have been observed for any ion at any pressure. These observations are in general agreement with calculations<sup>24</sup> which indicate that some of these halides do not possess an energy gap, and in those cases where no other experimental or theoretical evidence is available this work can be interpreted as showing that in these cases no energy gap exists.

Gap modes are observed for NaBr, NaI, KBr, and KI. Neutron-scattering studies have shown the existence of the energy gaps in NaI, KBr, and KI, and the observed gap modes are found to be located fairly centrally within these gaps. Karo and Hardy<sup>24</sup> have calculated that an energy gap exists in NaBr, but our gap modes (117–127  $\text{cm}^{-1}$  for  $\text{NCO}^-$  and 110–123  $\text{cm}^{-1}$  for  $\text{CN}^-$ ) suggest that the gap is wider and at a higher energy than that calculated by them.

Torsional motion of the impurity ion seems to play an important part in most of the gap modes found for polyatomic impurity ions.

The gap modes in KBr and KI are not replaced by any equivalent structure when these halides are compressed into their high-pressure (CsCl-type) structure. No gap modes are found in the high-pressure external-mode spectra of the rubidium halides. Thus we feel confident in stating that there are no energy gaps in these materials in their high-pressure phases.

The pressure dependence of the gap-mode frequencies, especially for KBr, where the gap is very narrow, has been used as a guide to the pressure dependence of the bordering host-lattice frequencies.

#### External Modes within the Optic Bands of the Host Lattice

With only one exception, discussed below, only relatively broad features are found in the external-mode sidestructure in the energies covered by the host-lattice optic bands. These broad external-mode features

have been used to indicate the extent of the host-lattice band, but their detailed interpretation clearly requires a refined theoretical investigation.

The one band under this heading which was found to become very sharp at very low temperatures is the 154- $\text{cm}^{-1}$  (at 100°K) band in  $\nu_{\text{ext}}$  for  $\text{CN}^-$  in NaBr. No explanation for this band is suggested, but it is seen as highly significant that this band is found, for the  $\langle 001 \rangle$ -oriented  $\text{CN}^-$ , at a frequency which corresponds to a marked low-absorption region for the  $\langle 111 \rangle$ -oriented  $\text{NCO}^-$ .

#### Superoptic Local Modes

For the various polyatomic-impurity ions which we have studied, these modes, if they are found to exist, always seem to be interpretable in terms of a torsional motion of the impurity. In many cases, one of these modes is found to be very close, and possibly coincident with, the highest optic-mode frequency of the pure lattice. Superoptic modes, if they are to exist at all, must be quite highly localized. One requirement for their existence is therefore that the nearest neighbors alone must be sufficiently massive to represent an adequate counterbalance (stationary center of gravity and zero net angular momentum) without themselves having too large an amplitude, thus involving another shell of ions. The failure of the six nearest-neighbor sodium ions to comply with the above condition is considered to be the main reason why no such modes have been found for our relatively massive impurities in the sodium halides.

Mainly the lattice-sideband structures shown in Figs. 7 and 8 have been used in the above discussion, but complementary information for other ions (see, e.g., Refs. 3–6) could be included to substantiate the above conclusions and in some cases give closer limits on phonon band gap energies and high-energy maxima of optic bands.

Although most of the lattice-sideband spectra which have been discussed have been due to impurity ions in alkali halides, some of the wider applications of this type of spectrum, and its pressure dependence, have been indicated.

#### ACKNOWLEDGMENTS

We are grateful to Professor W. C. Price, F. R. S., for laboratory facilities and encouragement. One of us (M. A. C.) is indebted to the Science Research Council for a maintenance grant, and we are grateful for financial assistance from the U. S. Army (Contract No. DA-91-591-EUC) and the Institute of Petroleum Hydrocarbon Research Group.